



2016-12-01

The Role of Viral Interleukin-6 in Tumor Development of Kaposi's Sarcoma-Associated Herpesvirus Lymphomas

Rebecca A. Fullwood
Brigham Young University

Follow this and additional works at: <https://scholarsarchive.byu.edu/etd>



Part of the [Microbiology Commons](#)

BYU ScholarsArchive Citation

Fullwood, Rebecca A., "The Role of Viral Interleukin-6 in Tumor Development of Kaposi's Sarcoma-Associated Herpesvirus Lymphomas" (2016). *All Theses and Dissertations*. 6194.
<https://scholarsarchive.byu.edu/etd/6194>

This Thesis is brought to you for free and open access by BYU ScholarsArchive. It has been accepted for inclusion in All Theses and Dissertations by an authorized administrator of BYU ScholarsArchive. For more information, please contact scholarsarchive@byu.edu, ellen_amatangelo@byu.edu.

The Role of Viral Interleukin-6 in Tumor Development of
Kaposi's Sarcoma-Associated Herpesvirus
Lymphomas

Rebecca A. Fullwood

A thesis submitted to the faculty of
Brigham Young University
in partial fulfillment of the requirements for the degree of
Master of Science

Bradford K. Berges, Chair
Brian D. Poole
Kim L. O'Neill

Department of Microbiology and Molecular Biology
Brigham Young University

Copyright © 2016 Rebecca A. Fullwood

All Rights Reserved

ABSTRACT

The Role of Viral Interleukin-6 in Tumor Development of Kaposi's Sarcoma-Associated Herpesvirus Lymphomas

Rebecca A. Fullwood

Department of Microbiology and Molecular Biology, BYU
Master of Science

Kaposi's sarcoma herpesvirus (KSHV) is a cancer-causing virus, primarily affecting AIDS patients. KSHV is found in 3-10% of the U.S. population and can cause a range of cancers in the highly immunosuppressed; these cancers include Kaposi's sarcoma, pleural effusion lymphoma (PEL) and multicentric Castleman's disease (MCD). The current techniques for treating these cancers are relatively ineffective, largely due to their inefficiency at targeting tumors formed by the infection. One protein produced by KSHV, the viral homolog of interleukin-6 (vIL-6), is thought to play a major role in tumor development post-infection. Here a novel animal model is implemented to study the ways vIL-6 affects tumor development through growth factors and other cytokines within infected highly immune-deficient Rag2^{-/-}γc^{-/-} mice. Mice were subcutaneously injected with one of three types of cells: B cells infected with a wild-type (WT) KSHV, B cells infected with mutant KSHV without the gene for viral interleukin 6, and a negative control of uninfected B cells. After allowing time for tumors to develop the mice were sacrificed and the tumors assessed. Analysis of the physical properties of the tumors, as well as markers expressed by the tumors, were used to help determine whether vIL-6 could be an appropriate target when treating these cancers. In this study vIL-6 was seen to influence certain B cell markers (CD30), as well as onset of tumors (with no significant increase in overall tumor mass, but with marginally statistically significant increase in tumor number). This indicates that although vIL-6 could play a small role as a target for cancer, further investigation into the relationship of CD30 in these types of cancers needs to be explored. It was also found that the KSHV viral-infection decreases the development of tumors compared with uninfected immortalized B cells (BJAB). Not only would results from this experiment help develop new treatments, and change the lives of those suffering with cancers induced by KSHV, but they would provide a foundation for future studies with these types of cancers.

Key Words: Kaposi's sarcoma-associated herpesvirus, KSHV, viral interleukin-6, cancer, lymphoma

ACKNOWLEDGEMENTS

I would first like to thank my advisor Dr. Berges of the Microbiology Department at Brigham Young University. Not only did he provide the fire and direction needed to inspire this research, but his door was always open as I experienced the failures and successes that research inevitably produces.

I must also express my very profound gratitude to the Simmons Center of cancer research of Brigham Young University for providing me with funding that enabled me to further dedicate myself to the pursuit of this project.

Finally, to my parents and spouse for providing me with constant support and unceasing encouragement through the process of researching and writing this thesis and throughout my years of study. This body of work would not have been possible without them.

Thank you.

TABLE OF CONTENTS

TITLE PAGE	i
ABSTRACT	ii
ACKNOWLEDGEMENTS	iii
TABLE OF CONTENTS	iv
LIST OF TABLES	vii
LIST OF FIGURES	vii
Introduction.....	1
Background.....	1
Herpesviruses.....	2
KSHV	3
KSHV Cancers	4
Viral Interleukin-6 (vIL-6)	6
Materials and Methods.....	11
A. Cells and viruses.....	11
B. Mouse injections.....	12
C. Histology	13
D. Flow cytometry.....	13
Chapter 1	15

Results	15
Analysis of number and mass of tumors extracted.....	15
Comparison of expression profiles for KSHV Δ vIL-6 and KSHV WT cells grown in culture	16
Comparing expression profiles of KSHV WT-infected cells grown in culture vs those extracted from tumors	18
Comparing expression profiles of KSHV Δ vIL-6-infected cells grown in culture vs those extracted from tumors	18
Comparing expression profiles of KSHV Δ vIL-6 and KSHV WT cells extracted from tumors	19
Discussion	29
Tumor Analysis	29
Impact of KSHV Δ vIL-6 gene on human B cell markers in culture	30
Impact of vIL-6 on B cell makers in both KSHV Δ vIL-6 and KSHV WT-infected cells after tumor development.....	30
Impact of KSHV Δ vIL-6 gene on human B cell markers in cells extracted from tumors	31
Summary.....	32
Chapter 2.....	33
Results	33
Tumor Analysis	33
Comparison of expression profiles for uninfected immortalized BJAB cells and KSHV WT-infected BJAB cells in culture.....	34

Comparing expression profiles of immortalized BJAB cells grown in culture vs those extracted from tumors	35
Comparing expression profiles of KSHV WT-infected cells grown in culture vs those extracted from tumors	36
Comparing expression profiles of uninfected BJAB cells and KSHV WT-infected BJAB cells extracted from tumors.....	37
Discussion	43
Analysis of Tumors	43
Impact of KSHV on human B cell markers in culture	43
Impact of KSHV on B cell makers in both infected and uninfected cells after tumor development	44
Impact of KSHV on human B cell markers in cells extracted from tumors.....	45
Summary.....	45
Conclusion	46
References.....	48
Appendix.....	58

LIST OF TABLES

Table 1: Raw tumor data.....	58
------------------------------	----

LIST OF FIGURES

Figure 1. The JAK/STAT signaling pathway.	10
Figure 2. vIL-6 affects the number of tumors derived from KSHV-infected mice outside of 95% confidence.	21
Figure 3. vIL6 does not affect the mass of tumors in KSHV-infected mice.	22
Figure 4. FACS analysis of propidium iodide negative, GFP+, CD30+ populations.....	23
Figure 5. FACS analysis comparison of cultured KSHV Δ vIL-6 –infected BJAB cells and KSHV WT-infected BJAB cells.....	24
Figure 6. Histogram of the CD30+ population comparing KSHV WT and KSHV Δ vIL-6.	25
Figure 7. FACS analysis comparison of cultured KSHV WT-infected BJAB cells and those extracted from tumors.	26
Figure 8. FACS analysis comparison of cultured KSHV Δ vIL-6-infected BJAB cells and those extracted from tumors.....	27
Figure 9. FACS analysis comparison of KSHV Δ vIL-6 –infected BJAB cells and KSHV WT-infected BJAB cells extracted from tumors.....	28
Figure 10. KSHV does not affect the number of tumors derived from injected mice.....	38
Figure 11. KSHV impacts mass of tumors in immortalized BJAB and KSHV WT-injected mice.	39
Figure 12. FACS analysis comparison of cultured immortalized BJAB and KSHV WT-injected BJAB cells.	40

Figure 13. FACS analysis comparison of cultured immortalized BJAB cells and those extracted from tumors. 41

Figure 14. FACS analysis comparison of immortalized BJAB and KSHV WT-injected BJAB cells extracted from tumors. 42

Introduction

Cancer has justifiably been labeled “the emperor of all maladies.”¹ As the second leading cause for death in the United States² and with over 100 different variations affecting humans³, these abnormal growths of cells account for an unfathomable toll in individual suffering, along with expenses of \$1.2 trillion per year⁴. The scale and complexity of the disease presents a puzzle of gigantic proportions with millions of scientists each working to solve a small piece. Cancer research can focus on one or more areas of the sequence of events that accompanies the disease; these include agents that trigger genetic mutations in cells (such as viruses), the nature of the genetic modifications, and the resultant consequences to cell biology. This thesis attempts to make a small contribution to a specific area of the research effort that involves the role of agents, such as viruses, in the development of cancer. A deeper look at the specialized area of viral oncogenesis in humans is needed, with this research focusing on that of Kaposi’s sarcoma-associated herpesvirus (KSHV).

Background

Kaposi’s sarcoma-associated herpesvirus (KSHV), also known as human herpesvirus 8 (HHV-8), is a virus that causes cancer in highly immunocompromised individuals⁵. First diagnosed in 1872 as a slow-growing neoplasm in elderly men of the Mediterranean by Moritz Kaposi⁶, Kaposi’s sarcoma (KS) became a global concern when a more aggressive and rapidly fatal strain of the virus was identified amongst the homosexual populations in 1981^{7,8}. The virus went on to infect 15% of all registered acquired immune deficiency syndrome (AIDS) patients in the United States by 1989⁹, bringing about a dire need for stronger research into what was causing these illnesses and how best to treat them.

Although infections associated with the virus were becoming increasingly concerning amongst the scientific community, the agent causing this epidemic was not identified until 1994¹⁰. This has made it

one of the most recent oncogenic viruses to be studied. Loss of immune function caused by human immunodeficiency virus (HIV) leaves AIDS patients more susceptible to the oncogenic properties of this virus, which would not manifest in a healthy person¹¹. The potential for this virus to become oncogenic in compromised individuals can lead to serious cancers, and many times death for those already suffering with various infections due to AIDS.

In the following sections we briefly review the nature of herpesviruses in general, and more specifically the KSHV strain, and its role in cancer formation and propagation. Finally, we review the potential role of a specific protein, vIL-6, in facilitating cancer formation and growth. The main body of the thesis will investigate prospective correlations between KSHV-induced cancers and the presence of vIL-6 in susceptible cells. It is hoped that the search for such interactions during the cancer evolution will lead to new insights for potential control or eradication of this sub-family of cancer diseases.

Herpesviruses

Kaposi's sarcoma associated herpesvirus (KSHV) is one member of the larger herpesviridae family. Among the 130+ members of this family¹², nine are known to be human herpesviruses (HHV) that affect the populous. The genomes of these viruses are somewhat large (124-230kb), double-stranded DNA genomes, enclosed by an icosahedral capsid and an envelope^{13,14}. Having co-evolved with the human host for millions of years they have become highly adapted to infect and persist within the human body. The years of this coevolution have resulted in most of the human population being infected with a herpesvirus, even before leaving infancy; more than 90% of adults have been infected by at least one of these viruses, with a latent form of the virus remaining in the vast majority of people. The virus is usually transmitted through saliva^{15,16}, blood¹⁷, organ donation¹⁸, or sexual contact^{19,20}. These viral infections will generally persist within the human body throughout the life of the host as a result of various mechanisms used to evade the immune system. One of the main systems used by the virus to do this involves switching from

a lytic to a latent infection. Herpesviruses have the ability to actively infect and replicate in cells²¹, but when the viral load has increased to a high enough level, the virus is able to convert to a latent cycle²². This system allows the virus to bridge its genome with the human genome and stop producing viral proteins²³, giving the virus the opportunity to persist within the human host undetected. When this cycle is active, the viral genome can be replicated along with the host cell and ultimately avoid activating any immune response. Although the virus is able to persist within the human body throughout the life of the host, severe disease does not usually result unless the host immune system is suppressed or compromised.

KSHV

Human herpesvirus types are classified under three subfamilies: α , β , and γ . KSHV shares many of the same traits as other viruses within the herpesviridae family, including its fellow γ -herpesvirus, Epstein-Barr virus (EBV). This specific virus currently infects 3-10% of the U.S. population²⁴. It is a double-stranded DNA virus that packages its genome linearly inside a protein capsid; this is surrounded by tegument proteins and finally enclosed by a lipid envelope sequestered from the cell membrane from which it replicates. As with other members of the HHV family, one of the more important characteristics of this virus is the ability for KSHV to alternate between latent and lytic life cycles. In order to remain latent within the cell the viral genome circularizes and the resultant episome is tethered to the host's genome via the latency-associated nuclear antigen (LANA) protein²⁵. When the virus is ready to begin a lytic program, the *rta* gene is expressed and activates other genes related to the lytic phase²⁶. This includes production of various virally encoded cytokines and chemokines such as vIL-6 and other inflammatory proteins²⁷. These proteins are imperative to disorders associated with the virus, as the resultant inflammation increases cellular migration to the site of infection. Subsequently the different chemokines are able to fine-tune the types of cells that migrate to the infected cells²⁸. This allows for tuning of the microenvironment to avoid unfavorable cytotoxic reactions that would otherwise destroy infected or

damaged cells. The result is a perfect breeding ground for damaged cells to continue replicating, which often leads to cancer.

KSHV Cancers

There are three main types of cancers associated with the KSHV herpesvirus, including classic Kaposi's sarcoma (KS), primary effusion lymphoma (PEL), and the plasmablastic variant of Multicentric Castleman's disease (MCD) ²⁹⁻³². The physical manifestations of these three cancers involve lesions (the sarcomas), lymphocyte oncogenesis, and tumors (for the MCD types).

Kaposi's sarcoma (KS) is the classic form of KSHV-induced cancer, first found in 1872 by the Hungarian dermatologist Moritz Kaposi⁶. The discovery involved the dark sarcomas found inflicting elderly male patients in the Mediterranean³³. This sarcoma is an unusual multifocal neoplasm that contains several different cell types and is characterized by dark, purple lesions³⁴. After this form of KS was discovered, 3 other epidemiological variants of KS were investigated: endemic, AIDS-related, and iatrogenic³⁵, all of which are associated with KSHV.

Classic KS was the first documented variant of the KS type, infecting mainly HIV-negative elderly Mediterranean men. Endemic KS is a form more prevalent in mid to south Africa³⁶; this variant is more aggressive than the classic KS, usually affecting children³⁷. AIDS-related KS specifically targets the compromised immune systems of those suffering from AIDS³⁸. Iatrogenic KS occurs after donor recipients undergo therapy to suppress their immune system to prevent graft rejection³⁹. KS lesions occur throughout cutaneous as well as mucosal surfaces, lymph nodes, and visceral organs^{40,41}. Although usually latently infected, KSHV gene expression is found in 95% of these malignancies⁴², aiding diagnosis.

The second prominent cancer caused by KSHV is primary effusion lymphoma (PEL). For this particular variant, the detection of active KSHV gene expression has become a necessary part of diagnosing this

type of cancer⁷. PEL manifests as a malignant effusion of monoclonal B cells within the peritoneal, pleural, or pericardial space, which usually originates with the infection of B cells⁴³. Although PEL is commonly seen as diffused cells, a few cases of solid tumor PEL have been documented; when present, the tumors are located in lymph node tissues⁴⁴. These lymphomas make up 3% of all AIDS-related lymphomas, the average survival time after diagnosis being 6 months⁴⁵. This results from the facts that the KSHV infection is not only very aggressive, but the treatment options relating to this rapidly fatal cancer are extremely limited. Within PEL, KSHV remains largely latent, but a large genome copy number exists within the cell (50-150 copies)⁴⁶. The latency of the infection implies that a minimal number of proteins are actively expressed. During the latency phase, very few proteins are produced, one of which is vIL-6 (to be explained in the next section); 2–5% of PEL cells actively express this protein⁴⁷. Associated with the production of these viral cytokine proteins, KSHV-infected B cells are also seen to display mutated immunoglobulin genes, and late-stage B cell markers such as (CD30 and CD138)⁴⁸. This leads us to believe that these cells originated from post-germinal centers. Observing and understanding these characteristics is imperative in creating new targets for cancer treatment, and add more information to the study of this aggressive cancer.

A third cancer associated with KSHV is plasmablastic multicentric Castleman's disease (MCD). This is characterized by localized B cell proliferation and vascular proliferation in germinal centers, usually forming a solid tumor mass following KSHV infection. The virus is reported to be found within all HIV-positive MCD cases, as well as 40% of HIV-negative cases^{49–51}. It is most commonly seen in AIDS patients and transplant recipients due to the repressed immune systems of both. Similar to the PEL variant, 5–25% of infected cells express vIL-6 in MCD tumors and generally appear to have a higher number of productive KSHV infected cells than that of PEL⁵². The polyclonal plasmablastic form of MCD is

extremely aggressive in those co-infected with HIV^{53,54}, the progression of which is thought to be caused by the imbalance of cytokines such as IL-6, IL-12, and VEGF⁵⁵⁻⁵⁸.

Due to the limited insights into the KSHV infections, there are few options with which to treat them; clinicians typically use monoclonal antibodies to target B cells for destruction, but this method is not specific to tumor cells. This research hopes to investigate new relationships between cytokines produced by the virus and cancer development, which could potentially lead to a targeted treatment option.

Viral Interleukin-6 (vIL-6)

Similar to other herpesviruses, KSHV has managed to pirate various human genes into its own genome as it has evolved alongside its host. One of these homologs is viral interleukin-6 (vIL-6). This cytokine is actively produced within many KSHV-associated malignancies^{59,60}, with the highest levels detected in MCD patients⁵¹. The vIL-6 cytokine is encoded in ORF K2 of the KSHV genome. The protein shares a 25% amino acid identity with its homolog, human IL-6 (hIL-6), or in a 63% amino acid similarity⁶¹⁻⁶³. This indicates that there have been changes made to the gene throughout the history of the virus; leading us to assume that some functions of the protein may have been adjusted.

Within the human body, the IL-6 protein is used as a proinflammatory cytokine, gp130 signal enhancer, B cell proliferator, as well as an anti-inflammatory agent during muscle contraction⁶⁴. hIL-6 influences target cells by binding its IL-6 receptor (also known as gp80), as well as two transmembrane glycoproteins (gp130 homodimer)⁶⁵. Once this new complex has formed, dimerization leads to the activation of various signaling cascades. One of the most understood of these pathways is that of Janus kinase (Jak)³/STAT pathway⁶⁶. This signaling pathway is associated with various information transfers from outside of the cell to the cell nucleus, resulting in transcription and expression of genes for processes including differentiation, apoptosis and oncogenesis.

To control these pathways vIL-6 uses different methods than hIL-6. Although it is necessary for hIL-6 to bind both IL-6R and gp130 in order to trigger a signal cascade, this is not the case with vIL-6. It is not required for vIL-6 to bind both the gp130 subunit and the IL-6 receptor in order to activate cell signaling⁶⁷⁻⁶⁹, but when gp130 is bound, the signaling is enhanced^{70,71}. This indicates an ability for the virally produced cytokine to use whatever complex is available to activate signaling pathways. This may seem like a significant alteration between the hIL-6 and vIL-6, but it has been shown that vIL-6-gp130 binding is ~1000-fold lower than the hIL-6, IL-6R, and gp130 binding complex; making it less efficient as an extracellular cytokine than hIL-6⁴⁷. This indicates a loss of productivity to the protein when using this adjusted function.

Furthermore, although it seems that vIL-6 has some advantages in terms of the potential to stimulate gene expression in the absence of the IL-6 receptor, its secretion from the cell is less efficient than hIL-6. It has been seen that most vIL-6 remains localized in the endoplasmic reticulum (ER)^{72,73}; but with the help of gp130, the protein can be released into the rest of the cell⁷⁴. vIL-6 will not remain sequestered indefinitely, as the death of KSHV-infected cells could potentially trigger a substantial dump of vIL-6 into the surrounding tissue⁷⁵. These occasional bursts of vIL-6 could be due to active viral replication or cytotoxic T cell killing of infected cells. These different distributions of vIL-6 still result in the induction of cellular IL-6 expression into several cell-types⁷⁶, which goes on to play a role in the pathogenesis of KSHV.

Past research has also shown that host-encoded IL-6 is imperative in phenotypes associated with symptomatic KSHV infections. A study was performed on the transgenic expression of vIL-6 in mice, which resulted in hyperplastic germinal centers in the lymph nodes, plasmacytosis in the spleen, and other MCD-like phenotypes. These observations were absent in the IL-6 knock-out mice, leading us to conclude that mammalian IL-6 is essential to the mechanisms of vIL-6 during infection⁷⁷. Such conclusions begin

to build a picture of a dynamic and potentially complex role for vIL-6 in the oncogenic process that we hope to begin to unravel.

vIL-6 is expressed during both lytic and latent KSHV infections, which is unusual for virally produced cytokines. The fact that this protein is utilized throughout both types of life cycles indicates some important roles potentially associated with this protein. Some of these roles potentially involve the activation of similar signaling pathways to those triggered by the human IL-6 counterpart, such as JAK/STAT, MAPK, and PI3K/Akt pathways (**Figure 1**)^{78,79}. These pathways lead to the upregulation of hIL-6⁷⁶, VEGF, B cell proliferation, and other cytokines (IL-10 and IL-12)^{47,80,81}. It has been shown that *in vivo*, vIL-6 increases angiogenesis of tumors via VEGF (**Figure 1**), a growth factor known to increase angiogenesis and endothelial cell invasion^{82,83}. Increased vascularization would allow tumor cells to remain more viable and provide the virus a greater access to the environment around the tumor. B cell proliferation is also advantageous to the virus, as the virus primarily infects B lymphocytes. This allows the virus to access a larger population of cells to infect and subsequently replicate within.

The purpose of this project is to further understand the role of vIL-6 in Kaposi's sarcoma herpesvirus (KSHV) tumor development. Viral interleukin 6 is currently thought to aid tumor growth by upregulating proteins which promote angiogenesis, B cell proliferation, and anti-apoptosis signals⁷². ***Our hypothesis is that viral interleukin-6 is necessary for tumor development in larger tumors such as those found in MCD; therefore, when present, it is expected to increase tumor mass and promote angiogenesis as well as metastasis of the tumor.*** The hypothesis was tested by injecting B cells that are latently infected with KSHV into highly immunocompromised mice in order to analyze the effects of vIL-6 on tumor development. The technique of injecting KSHV-infected B cells both subcutaneously and into the intraperitoneal has been previously shown to produce tumors⁸⁰. By comparing tumors induced by KSHV, with and without the gene for vIL-6, it is possible to identify whether vIL-6 could be an effective target

for treating KSHV induced cancers. Not only does this thesis compare the physical characteristics of both tumors, such as mass, and total number of tumors, but it measures different cell marker levels which may indicate any effects that vIL-6 plays in tumor growth and development. Since classic Kaposi's sarcoma infections are cancers of the endothelial cells, we are unable to mimic this type of infection within a mouse model. Hence the investigation focuses on the role of vIL-6 in KSHV infections similar to PEL and MCD cancers.

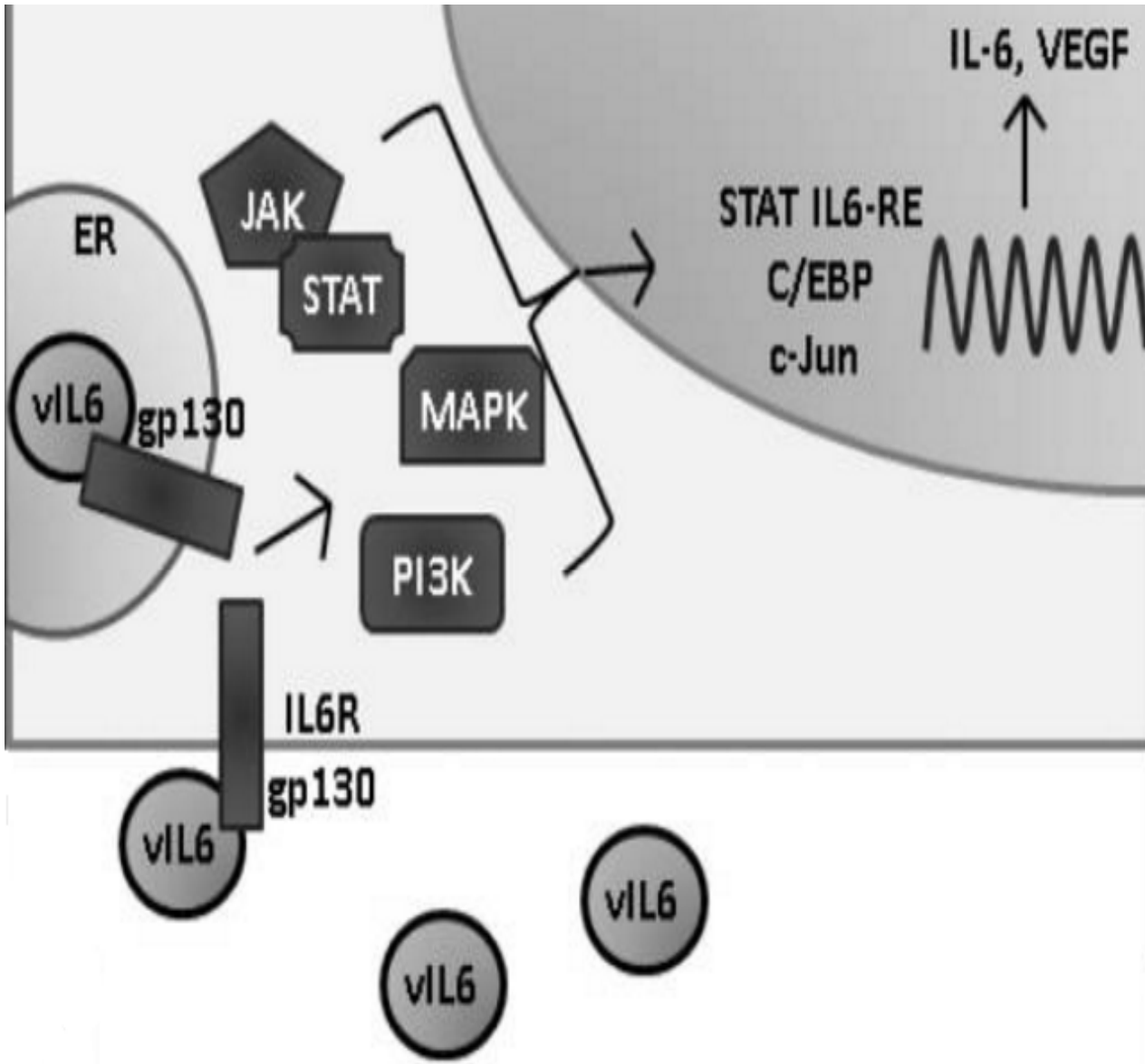


Figure 1. The JAK/STAT signaling pathway. This pathway can be stimulated by IL-6 using either the gp130 or the gp130-IL-6-complex (Source: KSHV: pathways to tumorigenesis and persistent infection by Giffin & Damania⁷⁹).

Materials and Methods

As described above, the purpose of the experimental procedure is to determine the influence of vIL-6 on KSHV induced tumor development. Various stages characterized the process of tumor formation and analysis. Healthy cell lines were infected with the desired viruses and cultivated. Mice were then injected subcutaneously over the abdomen with the different cell types, and tumors were allowed to develop for 5 weeks. Tumors were then extracted and analyzed for mass and frequency before phenotypes were documented via flow cytometry.

A. Cells and viruses

i. Cell types used

The desired virus and cells (BJAB, BJAB WT, and BJAB Δ vIL-6) were all supplied by Dr. Lagunoff (University of Washington). The first group of cells (BJAB) is simply the uninfected immortalized B cell line. The second group of cells (BJAB WT) included the KSHV wild-type virus. The virus is in the human B cell line, BJAB, in the form of a BAC construct containing the KSHV genome, GFP, and a puromycin resistance gene⁸⁴. The last group of cells (BJAB Δ vIL-6) contained a BAC constructed with a KSHV genome with 303 bases of the pKS11K2 vIL-6 reading frame removed by digesting *EcoRI* and *PstI*⁸⁵, GFP, and a puromycin resistance gene. All cells were recovered by defrosting the pre-frozen samples before adding 14mL of PBS in order to dilute the dimethyl sulfoxide (DMSO) that is used to protect the cells during the freezing process. This was then centrifuged at 3,000rpm for 3 minutes and the supernatant discarded. The cells were then grown in RPMI 1640 containing 10% fetal bovine serum (FBS), 100x penicillin/streptomycin, 2mM L-glutamine, and sodium bicarbonate. After mixing this solution the pH was adjusted to 7-7.2 to provide an ideal cell growth environment. The solution was filter-sterilized and warmed to 37°C before adding cells. Cells were seeded at a density of ~500,000 cells/mL; lower densities would keep the cells from thriving within the media. Cells were then be incubated at 37°C, 5% CO₂. After

allowing the cells to revive and begin growth within the media for over 24hrs we added a 1:100 dilution of 10mg/mL puromycin to the RPMI media of both solutions of virally-infected cells and passaged for one month to select for puromycin-resistant GFP⁺ cells. We maintained healthy stocks of BJAB, BJAB with wild-type KSHV, and BJAB with KSHV Δ vIL-6 cells until 80% of virally-infected cells were GFP⁺ (as confirmed using flow cytometry).

ii. Cell verification

Before injection all cell types were stained with propidium iodide in order to assess the percentage of live and dead cells. GFP positive cells were monitored and selected for until at least 80% of cells expressed the gene.

B. Mouse injections

It had been previously shown that injection of 5×10^6 KSHV-infected B cells causes visible tumors via subcutaneous injection in 2 out of 3 SCID mice⁸⁰. We decided to use the more immune-deficient Balb/c Rag2^{-/-} γ c^{-/-} mouse strain so as to guarantee tumor development. Once the cells were grown to the desired concentration, 5×10^6 live cells from each group were centrifuged and re-suspended in 40 μ L of Iscove's Modified Dulbecco's Medium (IMDM). Using a BD 28 – gauge needle, each mouse, aged between 8-15 weeks old, was injected subcutaneously, directly over the abdomen. The needle remained in place for 30 seconds after injection, and was slowly removed (10s). An initial 6 mice per study group were used, 3 males and 3 females; the experiment was then repeated, resulting in 12 mice per study group, and a total of 36 mice. Animals were monitored for changes in health for 5 weeks.

Hazards throughout the process were minimized by using standard procedures and IACUC protocols. The BYU Institutional Animal Care and Use Committee approved our proposal to begin this research (protocol # 15-0108).

C. Histology

***i.* Harvesting tumors**

After 5 weeks tumors were identified and the animals were sacrificed consistent with recommendations from the Panel on Euthanasia of the American Veterinary Medical Association. Mice were dissected and the tumors excised. The total number of tumors, as well as individual and total tumor mass per animal were recorded. Tumors were then cut in two. One of half of each tumor per mouse was placed flat in a plastic mold before being covered with optimum cutting temperature (O.C.T) compound (Tissue-Tek Fischer Medical Company) and stored at -80°C. The rest of the tumors were separated into individual cells using a plunger from a 10mL syringe (BD), 1 X PBS, and a 40µm Cell Strainer (BiolGix Research Company). These cells were then set aside for flow cytometry.

***ii.* Slide preparation**

Tumor tissue samples were prepared for staining by using the Microm HM550 to mount 12µm tumor sections onto Superfrost Plus, positively charged white slides (Thermo Scientific). O.C.T covered tumors were removed from -80°C and the blocks mounted at -21°C using more O.C.T compound. These were then left for a minimum of 20 minutes to allow the tissue sample to reach a stable temperature. The sections were then cut at -19°C to a thickness of 12µm before mounting onto the slide. These samples were left to fix at room temperature for 30 minutes before storing long-term at -80°C.

D. Flow cytometry

In order to analyze the expression profiles of both cultured cells and those extracted from the tumors, 200,000 live cells were counted and collected using a hemocytometer, the supernatant removed, and the cells re-suspended in 100µL of FACS stain buffer. 3µL of Mouse/Human Fc block was added and incubated at 4°C for 15 minutes. 3µL of the desired antibody was added and incubated for 30 minutes at 4°C. The cells were then fixed by adding 1% paraformaldehyde up to 500µL. The cells were then

centrifuged for 3 minutes at 3,000rpm, the supernatant removed, and the cells re-suspended in 500 μ L of 1X PBS. Due to the different light frequency requirements of the antibodies used, it was necessary to run the analysis via 2 panels. Panel A: CD45 (PE-cy7), CD19 (APC-e-Fluor780), CD20 (APC), CD138 (PE-cy5.5), CD22 (PE). Panel B: CD19 (APC-eFluor780), CD38 (PE-cy7), CD30 (APC). Unstained controls of both BJAB and BJAB KSHV WT cells were also analyzed for contrast with the stained cells.

Chapter 1

Results

No suitable animal study has extensively investigated the behavior of vIL-6 in regards to tumor development *in vivo*. Previous research has proved that injected BCBL-1 cells, harboring latent KSHV into Rag2^{-/-}γc^{-/-} mice, results in the development of vascularized tumors; similar results were expected here with different KSHV strains⁸⁰. Physical characteristics of tumors grown in the presence or absence of vIL-6, as well as investigations into gene expression that could be affected by vIL-6 were assessed after tumor formation.

The hypothesis underlying this thesis is that the presence of vIL-6 will promote growth of tumors. In fact, the results of the tests on the twelve mice demonstrated no statistically significant difference in the tumor rate of growth. The detailed results are summarized below, and the potential causes are analyzed in the context of expression profiles measured for each cell type.

Analysis of number and mass of tumors extracted

As outlined in the methods section, cells with and without the vIL-6 were grown in culture until both populations showed 80% or more GFP expression. The Balb/c Rag2^{-/-} γc^{-/-} mice were then injected with 5x10⁶ live cells from each group of cultured cells, subcutaneously, directly over the abdomen. The mice were monitored for 5 weeks before the tumors were extracted, analyzed, and further FACS experimentation performed on the cells derived from the tumors. All tumors of visible size were removed; most often these were easily extracted from the intraperitoneal space using tweezers, although some had formed subcutaneously, and required surgical removal before analysis.

The mass of each tumor was recorded, and an assessment was made of the significance of any variation in tumor growth between the two cases. In general, the mice injected with the cells that contained vIL-6

(KSHV WT) had more tumors (up to a maximum number of 4) but of lower average mass than those from the mice with the protein deficient cells. This potential difference in tumor behavior is highlighted in a comparison of total mass and number of tumors in order to determine basic tumorigenesis of cells infected with KSHV with and without the vIL-6 gene.

Statistical analysis of this behavior found no significant difference between the number of tumors or the mass of tumors when comparing Δ vIL-6-infected mice and WT-infected mice (**Figure 2 & Figure 3**). However, WT-infected mice clearly exhibit a higher average number of tumors (**Figure 2**), by 1.538 tumors; the statistics are within 1% of statistical significance according to the typical 95 percentile analysis ($p=0.0592$).

Given that a more significant difference in response was predicted for the different mice, in order to explore the reasons behind this unexpected finding, a more detailed analysis of the expression profiles from the various cell types was undertaken. Seven cell markers were quantified, with particular focus on the CD30 marker to determine the potential influence of these factors on the results. Cells in the following categories were investigated and compared:

1. Cells with and without vIL-6 grown in culture (KSHV WT vs KSHV Δ vIL-6)
2. KSHV WT-infected cells before and after tumor development
3. KSHV Δ vIL-6-infected cells before and after tumor development
4. Cells with and without vIL-6 after tumor growth (KSHV WT vs KSHV Δ vIL-6)

Comparison of expression profiles for KSHV Δ vIL-6 and KSHV WT cells grown in culture

Differences in gene expression patterns between constructs containing KSHV with an intact vIL-6 gene (KSHV WT) vs those with a deleted vIL-6 gene (KSHV Δ vIL-6) were cataloged using flow cytometry. BJAB cell populations grown in culture were analyzed in order to determine any differences before

infecting the mice with KSHV, and we later performed similar experiments comparing cells extracted from tumors that developed inside of mice. We used the profiles taken of cultured cells and compared them to those that were extracted from tumors in order to determine if changes in gene expression took place during the process of tumor development.

Most experiments were directed at B cell markers because our BJAB construct is a human B cell line. GFP expression (viral constructs contain the GFP gene) also allowed verification that similar percentages of cells were infected with KSHV before the mice were infected (**Figure 4**).

Data on the seven quantified markers (**Figure 5A**) indicated several statistically significant observations. KSHV Δ vIL-6-infected BJAB cells displayed 7.7% more CD45+GFP+ ($p < 0.0001$); 3.6% more CD45+CD22+ ($p = 0.0098$); and 8.2% more CD45+CD138+ expressing cells ($p = 0.0002$) compared with KSHV WT-infected cells.

This dataset provided a baseline for comparison of these cell lines after tumor growth. The analysis shows that certain genes were expressed differently in cells depending upon the presence or absence of the vIL-6 gene. We then re-analyzed our results to examine the mean fluorescence intensity (MFI) of different cell surface markers. MFI measures the intensity of antibody binding to cellular markers, and so in addition to determining if a gene was expressed or not (**Figure 2A**) we also examined if genes were expressed at different levels by measuring the MFI (**Figure 5B & Figure 6**).

We found that the MFI (**Figure 5B**) of these populations showed a lower intensity in KSHV WT-infected BJAB cells compared with uninfected BJAB cells in CD45+GFP+ markers and CD45+CD22+ markers. The differences being 2.6×10^4 lower GFP ($p < 0.0001$) and 1.1×10^3 lower CD22 ($p < 0.0001$).

Comparing expression profiles of KSHV WT-infected cells grown in culture vs those extracted from tumors

Deviations from the initial profiles of KSHV WT-infected BJAB cells as a result of tumor growth were analyzed using FACS analysis. Cultured KSHV-infected cells contained higher frequencies (**Figure 7A**) of CD45+ markers; CD45+GFP+ markers; CD45+CD19+ markers; CD45+CD20+ markers; CD45+CD22+ markers; and CD45+CD138+ markers compared with cells collected from tumors of KSHV-infected mice. CD45 had a 12.40% decrease ($p < 0.0001$), GFP a 52.33% decrease ($p < 0.0001$), CD20 a 27.41% decrease ($p = 0.0009$), CD22 a 36.56% decrease ($p < 0.0001$), and CD138 a 10.47% decrease ($p < 0.0001$) in tumor cells. CD45+CD30+ expression was upregulated in KSHV-infected tumor cells by 13.66% ($p < 0.0001$). There are a significant number of decreased markers following tumor growth in the case of KSHV WT-infected cells, with the percent of CD30+ cells increasing.

Mean fluorescence intensity of cultured KSHV WT-infected cells (**Figure 7B**) showed higher intensities for CD45 markers by 7.7×10^4 ($p < 0.0001$); CD45+GFP+ by 9.3×10^4 ($p < 0.0001$); CD45-GFP+ by 4.3×10^4 ($p = 0.0006$); CD45+CD19+ markers by 4.6×10^4 ($p < 0.0001$); CD45+CD20+ markers by 4.4×10^4 ($p < 0.0001$); CD45+CD22+ markers by 1.4×10^3 ($p < 0.0001$); and CD45+CD30+ markers by 1.6×10^4 ($p = 0.0127$) compared with KSHV-infected tumor cells. The MFI of most markers show a significant decrease in intensity post tumor-development.

Comparing expression profiles of KSHV Δ vIL-6-infected cells grown in culture vs those extracted from tumors

After the tumors developed and cells extracted, we were capable of analyzing any differences that occurred to the expression profiles of Δ vIL-6-infected cells due to tumor growth, based upon the baseline established in the previous section.

Figure 8A captures the relevant data, with significant results as follows: KSHV Δ vIL-6-infected cultures showed increases in frequency of CD45+ populations by 20.65% ($p < 0.0001$); CD45+GFP+ markers by 56.93% ($p < 0.0001$); CD45+CD19+ markers by 0.43% ($p = 0.0117$); CD45+CD20+ markers by 27.95% ($p < 0.0001$); CD45+CD22+ markers by 39.03% ($p < 0.0001$); and CD45+CD138+ markers by 13.54% ($p = 0.0111$) compared with uninfected BJAB cells. CD45-GFP+ markers increased by 6.062% ($p = 0.0244$) and CD45+CD30+ markers increased by 35.28% ($p = 0.0003$) in KSHV Δ vIL-6-infected tumor cells. One significant observation that can be made is that most markers decrease in quantity after tumor growth; however, this is not true of the CD30 marker, which actually increases in frequency. This is particularly meaningful due to the potential correlation between CD30 presence and cancer growth highlighted by other researchers.

Figure 8B displays the mean fluorescence intensity of the various markers. Cultured BJAB cells showed higher intensities for CD45+ populations by 6.3×10^4 ($p < 0.0001$); CD45+GFP+ markers by 1.2×10^5 ($p < 0.0001$); CD45-GFP+ markers by 5.7×10^4 ($p = 0.0033$); CD45+CD19+ markers by 4.7×10^4 ($p < 0.0001$); and CD45+CD20+ markers by 4.1×10^4 ($p < 0.0001$) compared with uninfected BJAB cells. These results reinforce the general trend for reduction in marker presence for most markers. For CD30, the intensity has remained fairly constant, while the frequency has increased (as shown in the previous figure).

Comparing expression profiles of KSHV Δ vIL-6 and KSHV WT cells extracted from tumors

Differences in the expression profiles of cells infected with and without vIL-6 were expected. It was hoped that further analysis would explain the results of the significance found during the preliminary tumor analysis, as well as the general oncogenic mechanism of KSHV. **Figure 9A** displays the experimental data of marker frequencies found for KSHV WT and Δ vIL-6 populations after tumor development, the significant findings of which are summarized: KSHV Δ vIL-6-infected tumor cells were seen to have increased live (propidium iodine negative) GFP+ and live CD30+ markers by 20.54% ($p = 0.0442$) and

10.12% (p=0.0110) respectively compared to the KSHV WT infection. KSHV WT-infected tumor cells showed a higher frequency of CD45+ populations by 8.717% compared with KSHV Δ vIL-6-infected tumor cells (p=0.0206).

Mean fluorescence intensity of these populations showed, in **Figure 9B**, a lower intensity in KSHV WT-infected tumor cells compared with KSHV Δ vIL-6-infected tumor cells in live CD30+ markers by 1.5×10^3 (p=0.0485). This further verifies the decrease of CD30 seen in the previous finding.

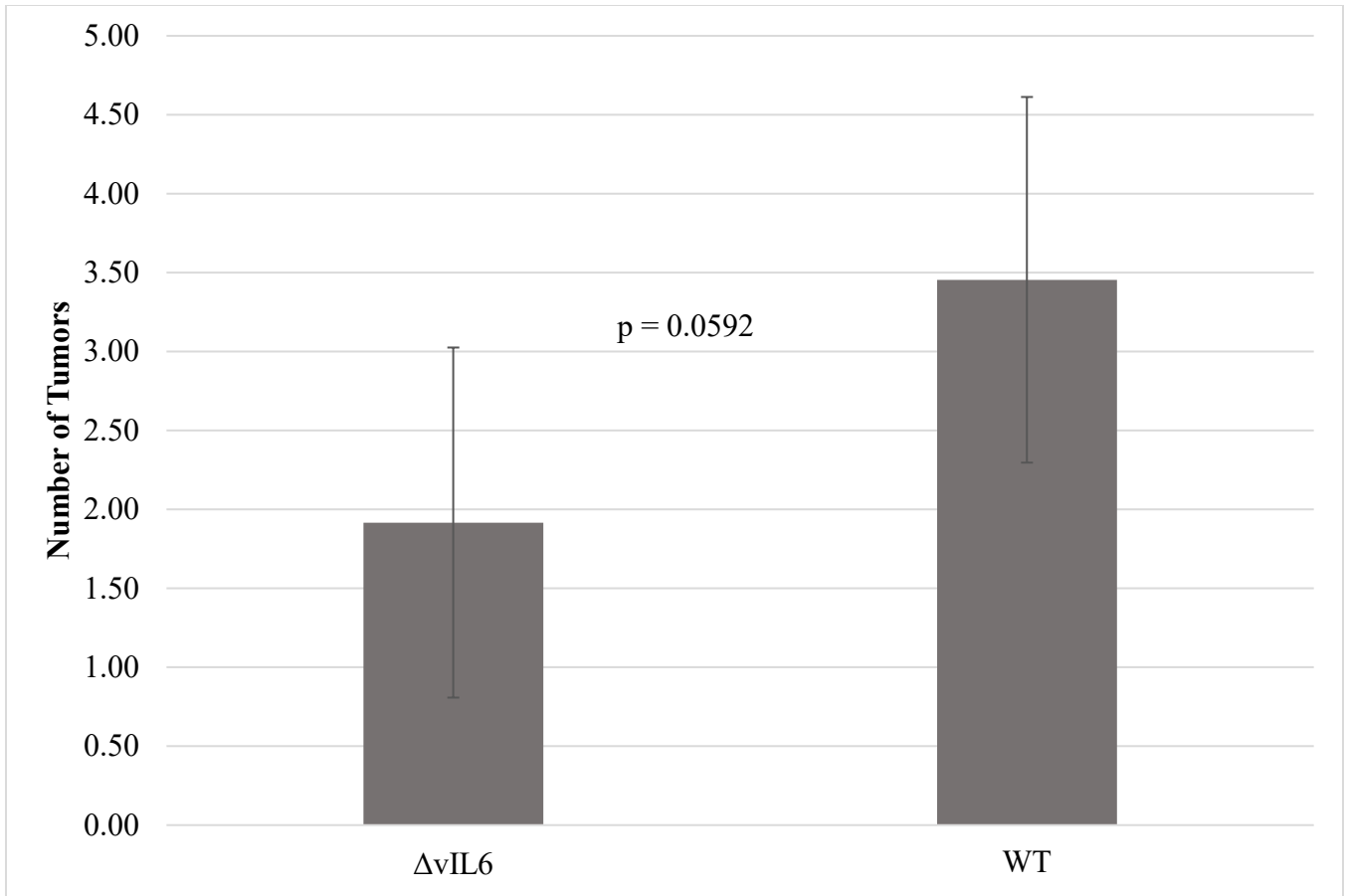


Figure 2. vIL -6 affects the number of tumors derived from KSHV-infected mice outside of 95% confidence. Each tumor was carefully excised from the mice and numbered at 5 weeks. The total number of tumors in each mouse from both groups was then analyzed (n=12, n=11).

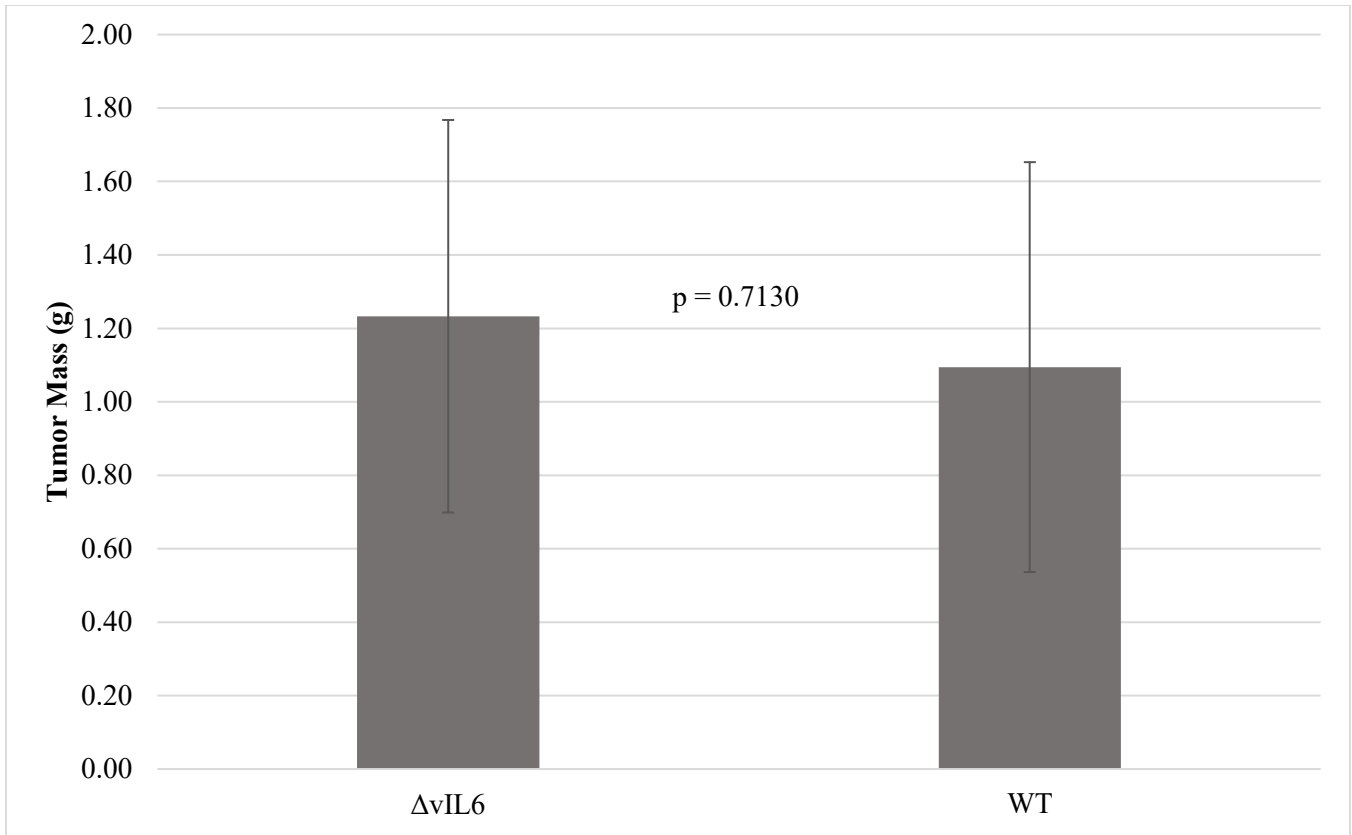


Figure 3. $vIL6$ does not affect the mass of tumors in KSHV-infected mice. Each tumor was carefully excised from the mice and weighed at 5 weeks. The total weight of each group was then analyzed (n=12, n=11).

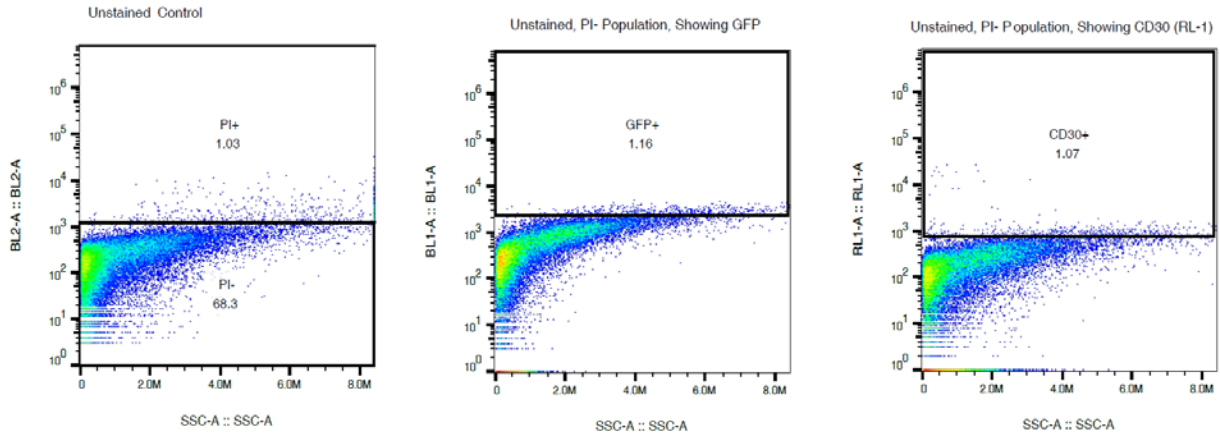


Figure 4. FACS analysis of propidium iodide negative, GFP+, CD30+ populations. Experiments were first gated on PI- markers, these PI- cells were then gated for GFP+ markers, finally PI-, GFP+ cells were gated for CD30+ markers and the results analyzed (this process was repeated for CD45+ populations that were analyzed.).

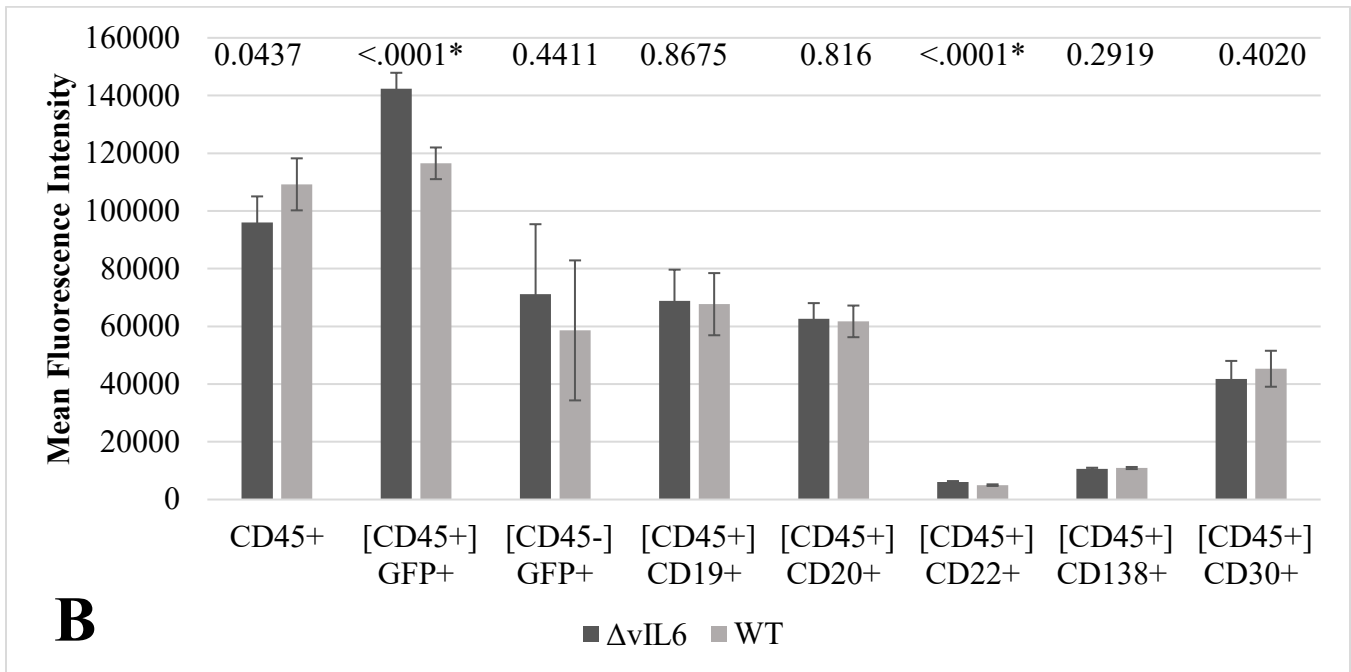
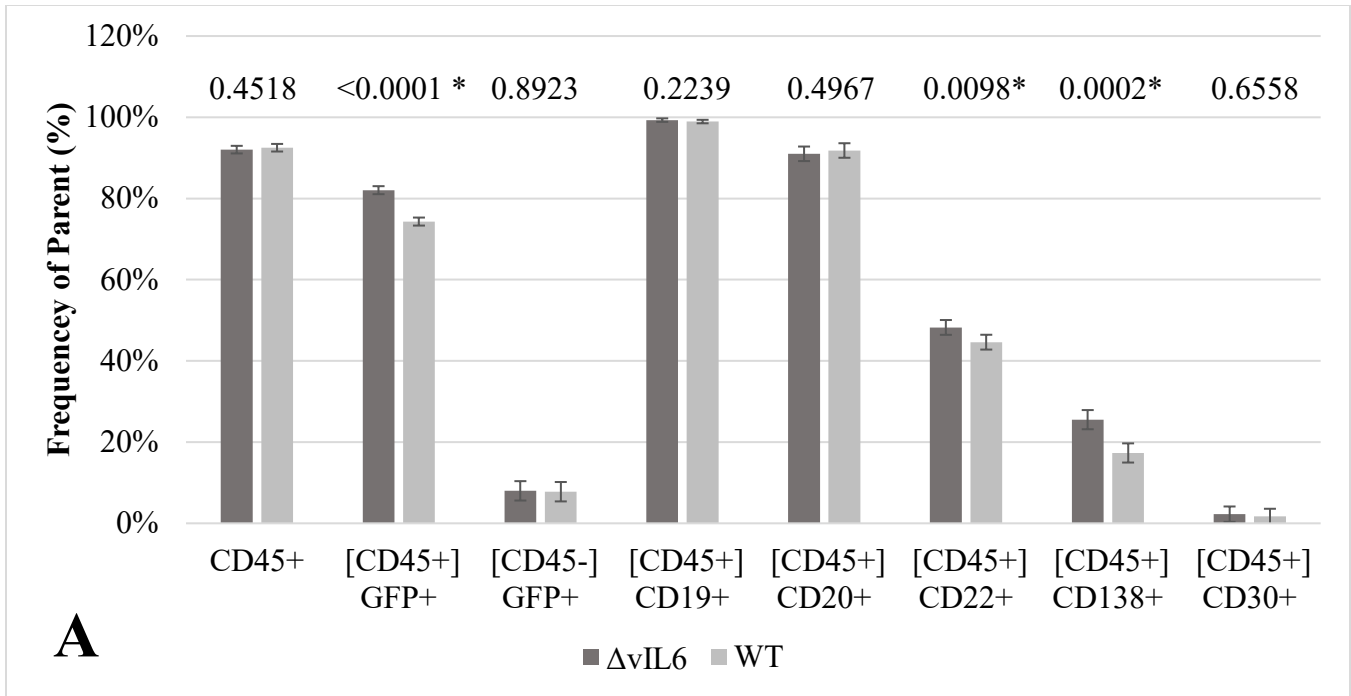


Figure 5. FACS analysis comparison of cultured KSHV $\Delta vIL-6$ –infected BJAB cells and KSHV WT-infected BJAB cells. A, Frequency of CD45+ cells, which display markers for GFP, CD19, CD20, CD22, CD138, and CD30; B, Mean fluorescence intensity of CD45+ cells, which display markers for GFP, CD19, CD20, CD22, CD138, and CD30. (* indicates a statistical significance less than $p = 0.05$ according to a pooled t-test analysis)

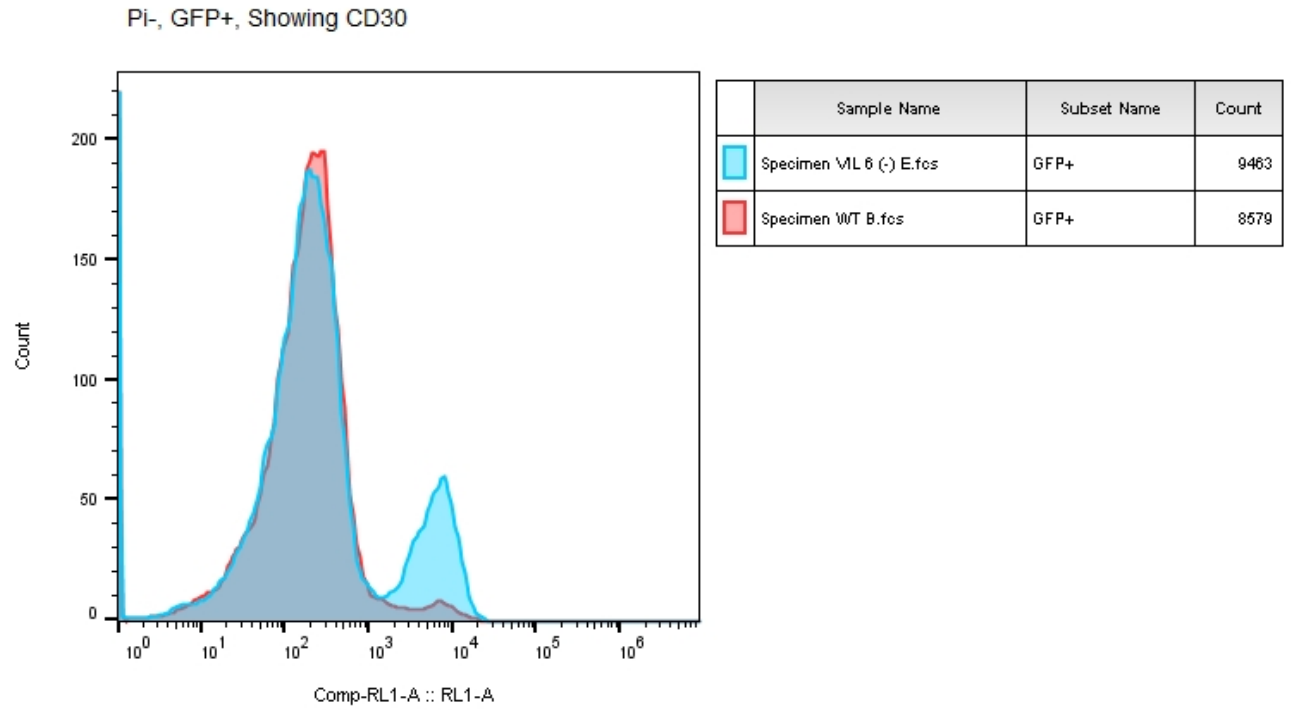


Figure 6. Histogram of the CD30+ population comparing KSHV WT and KSHV Δ iL-6. Overlay of CD30+ populations from mean KSHV WT and KSHV Δ iL-6-infected tumor cells.

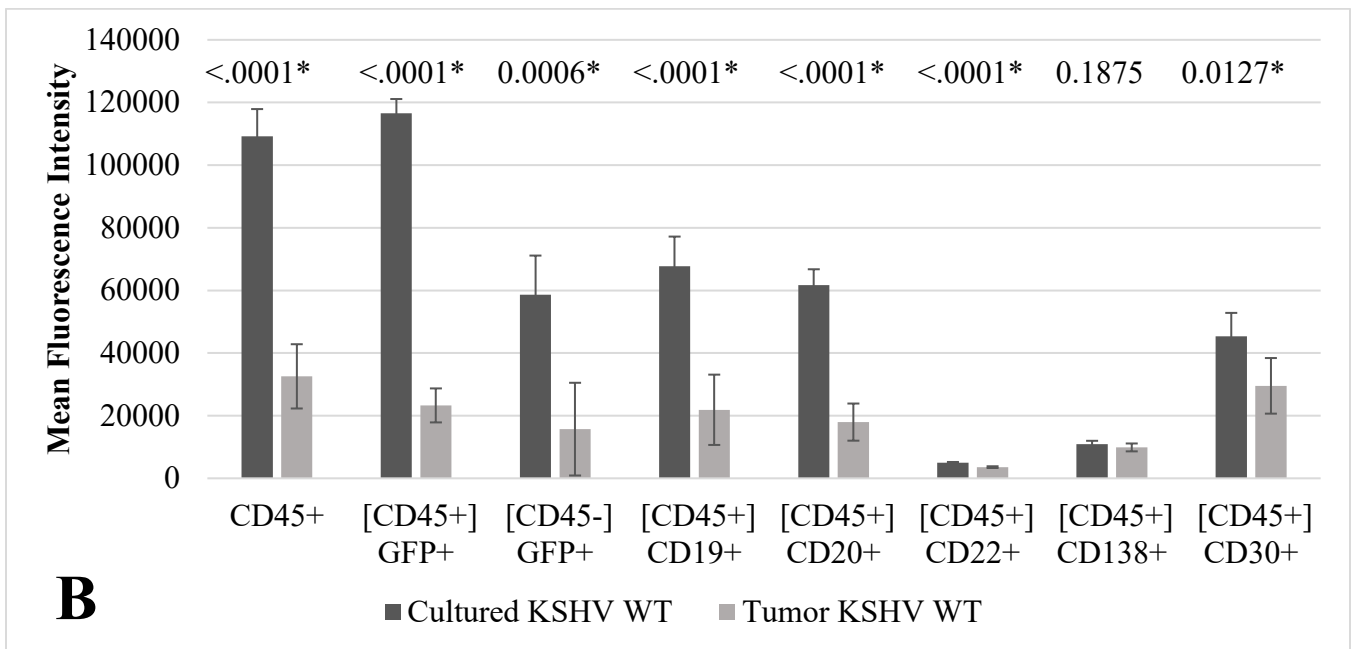
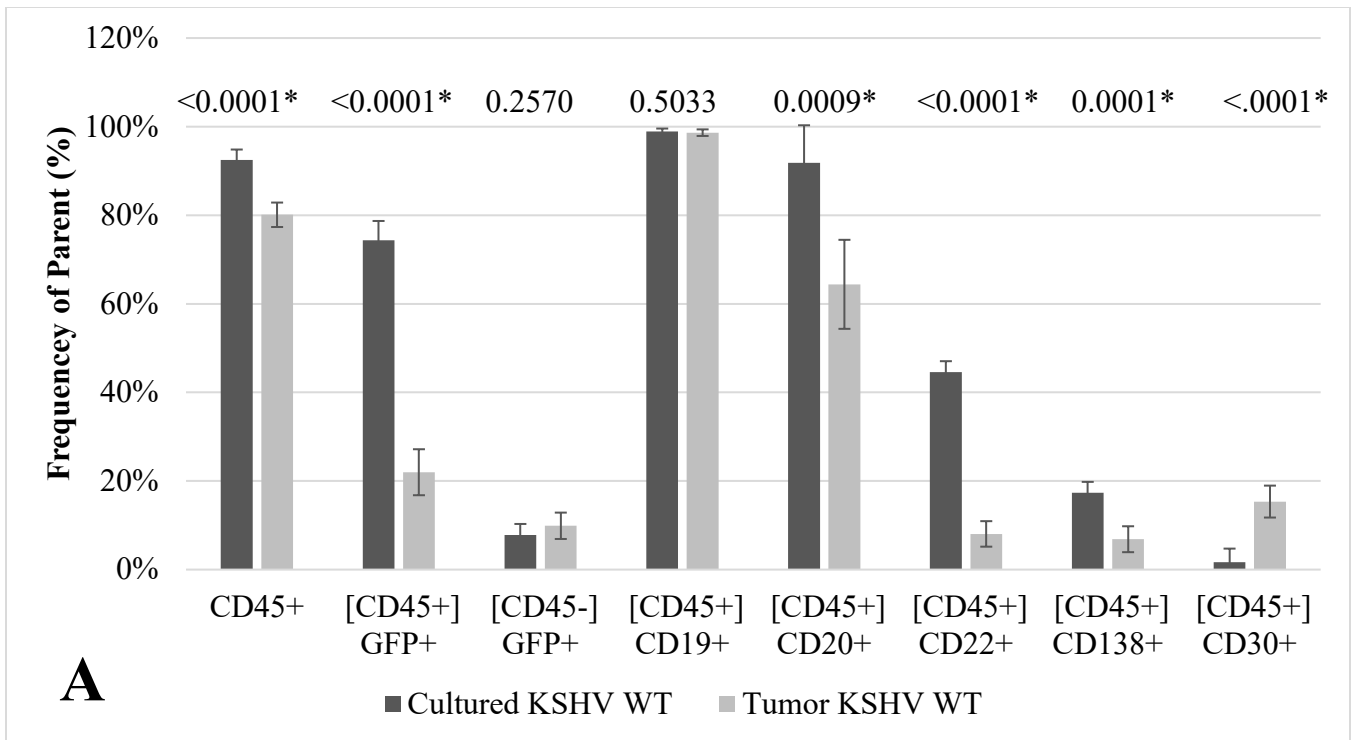


Figure 7. FACS analysis comparison of cultured KSHV WT-infected BJAB cells and those extracted from tumors. *A*, Frequency of CD45+ cells, which display markers for GFP, CD19, CD20, CD22, CD138, and CD30; *B*, Mean fluorescence intensity of CD45+ cells, which display markers for GFP, CD19, CD20, CD22, CD138, and CD30. (* indicates a statistical significance less than $p = 0.05$ according to a pooled t-test analysis)

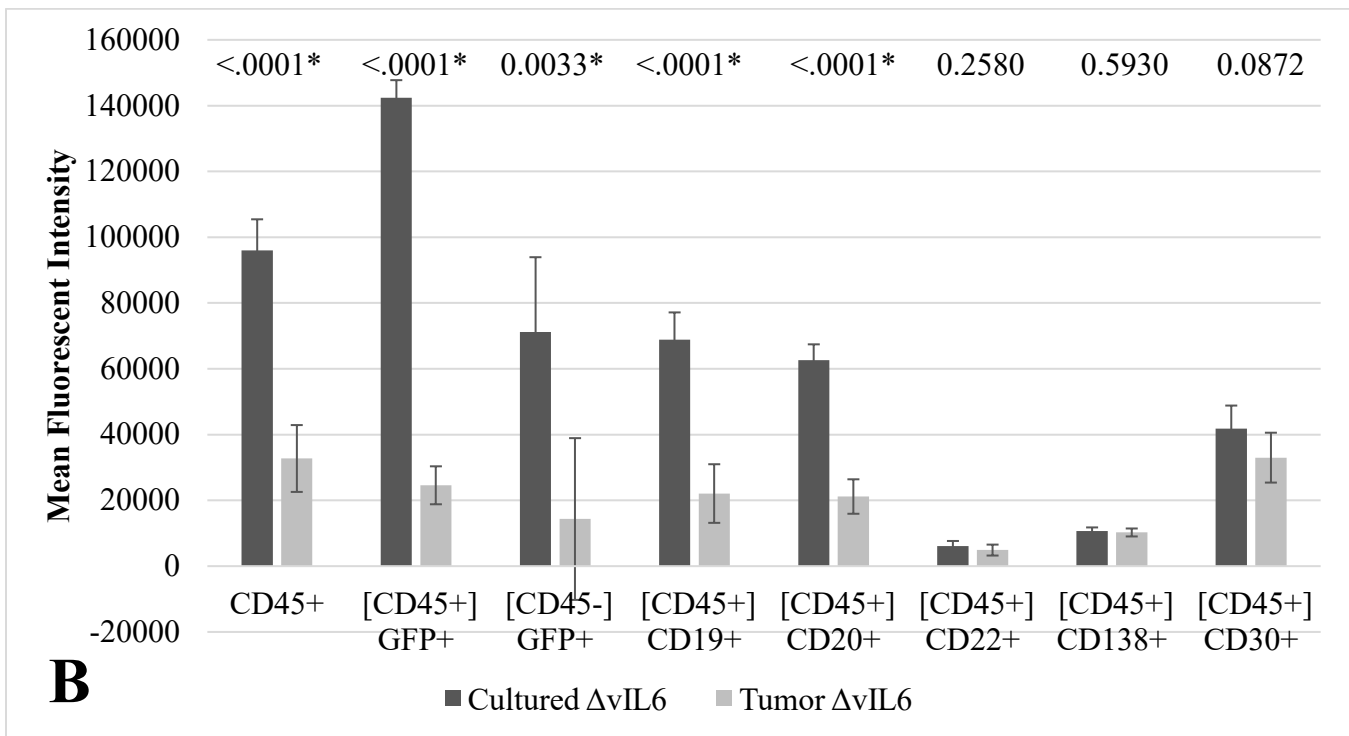
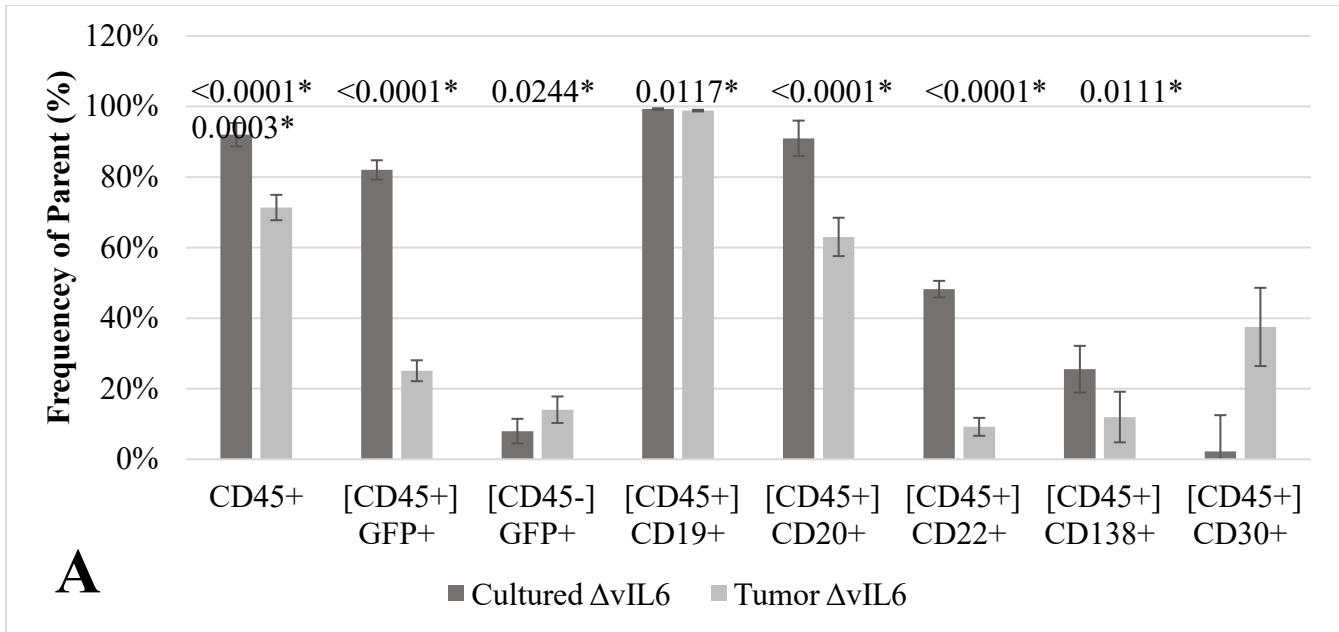


Figure 8. FACS analysis comparison of cultured KSHV $\Delta vIL-6$ -infected BJAB cells and those extracted from tumors. A, Frequency of CD45+ cells, which display markers for GFP, CD19, CD20, CD22, CD138, and CD30; B, Mean fluorescence intensity of CD45+ cells, which display markers for GFP, CD19, CD20, CD22, CD138, and CD30. (* indicates a statistical significance less than $p = 0.05$ according to a pooled t-test analysis)

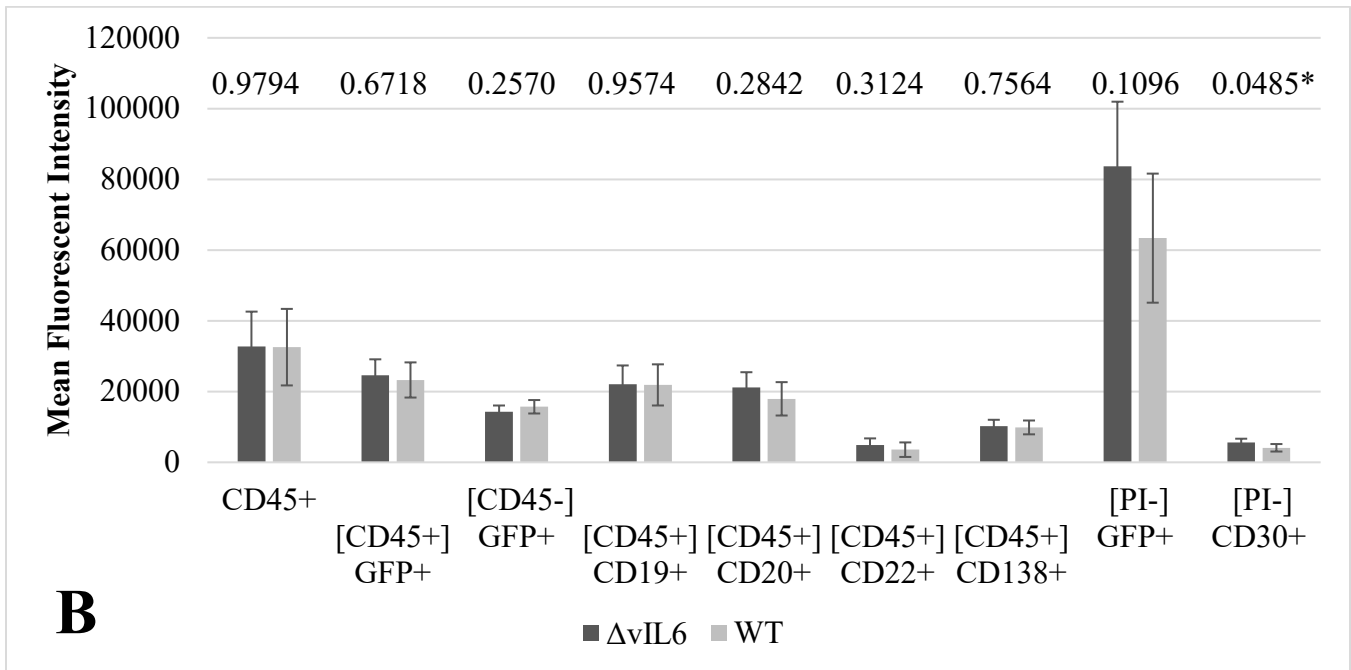
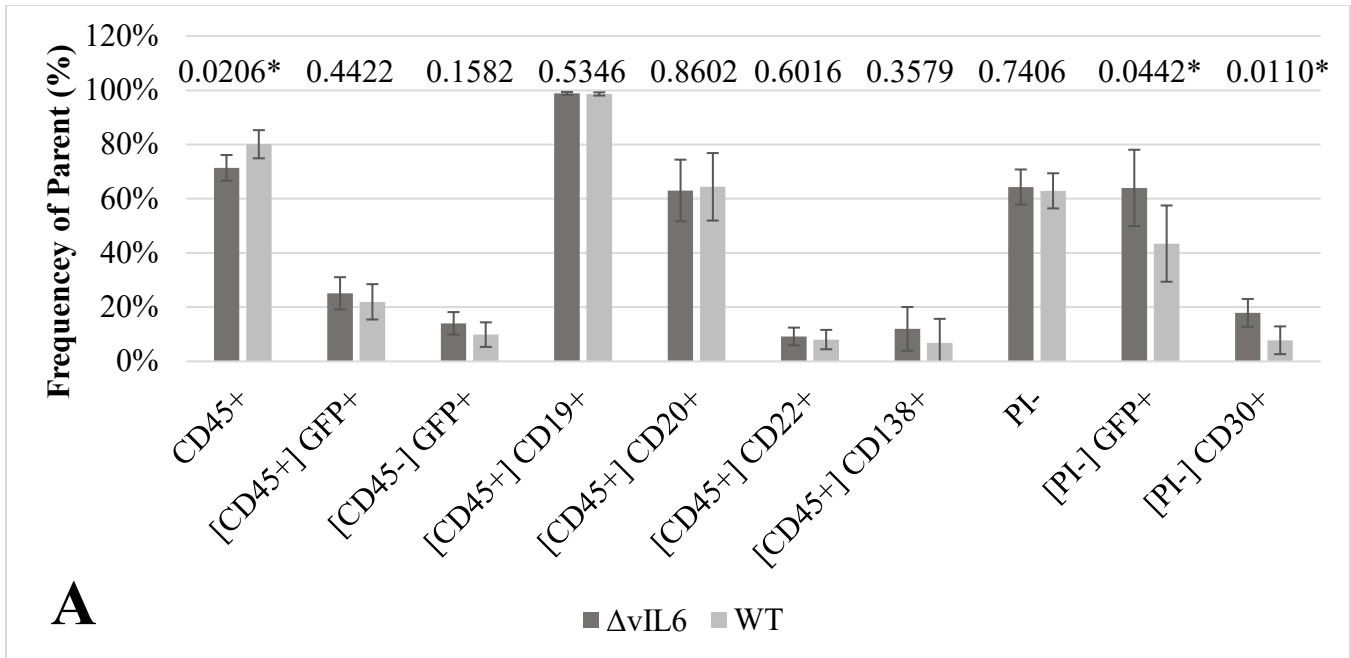


Figure 9. FACS analysis comparison of KSHV $\Delta vIL-6$ –infected BJAB cells and KSHV WT-infected BJAB cells extracted from tumors. A, Frequency of CD45+ and propidium iodine-negative populations, which display markers for GFP, CD19, CD20, CD22, CD138, and CD30; B, Mean fluorescence intensity of CD45+ cells, which display markers for GFP, CD19, CD20, CD22, CD138, and CD30. (* indicates a statistical significance less than $p = 0.05$ according to a pooled t-test analysis)

Discussion

The initial hypothesis proposed that the highest number of tumors and highest tumor mass should exist in the wild-type KSHV infected mice. This was based upon an extrapolation from previous research that showed an increase of blood flow due to the vIL-6 protein; hence feeding tumor growth via viral interleukin-6 being present throughout the tumor development. In contrast, it was expected that fewer and smaller tumors would occur within those mice infected with the mutant virus, due to the lack of vIL-6.

Tumor Analysis

From **Figure 2**, it is clear that more tumors are produced in the cells with the vIL-6 protein. When analyzed using a pooled T-test, the difference in number of tumors was outside of the margin for statistical significance (the calculated p-value was 0.059, while a statistically significant value would be below 0.05). Hence, while the number of tumors produced by KSHV WT-infected cells and KSHV Δ vIL-6-infected cells was not categorically significant using this particular statistical metric, the p-value was close to significant, leading us to believe that further investigation and more test subjects would potentially demonstrate that there is in fact a statistical correlation between the presence of the protein and the number of tumors that are produced.

However, from **Figure 3**, it is clear that the total mass of tumor has not significantly changed due to the presence or lack of the protein; i.e. vIL-6 does not assist in creating larger tumors. This indicates that vIL-6 may contribute to different stages of cancer progression in different ways. Models for cancer categorize the development of the ailment into various phases; the two relating most to our analysis being onset and progression⁸⁶. With this in mind, vIL-6 could be playing a prominent role in the onset of cancer – helping tumors initiate – as opposed to supporting the progression and subsequently increasing mass of the tumor. The combination of results indicates that vIL-6 potentially increases metastasis in WT KSHV versus

Δ vIL-6 KSHV, indicating that vIL-6 potentially increases the spread of KSHV throughout the body, increasing cancerous tumors within the host, but does not promote growth of the metastasized tumors.

While this result was weaker than desired, based upon the initial hypothesis, it only provides one view of the tumor growth process, at the macroscopic level. A more in-depth analysis of tumor development at the cell level is possible via quantification of markers associated with the cancer cells from each experiment. The markers that we examined included: CD19+, a B cell marker; CD20+, a B cell marker that aids in differentiation into plasma cells; CD22+, a regulatory molecule of B cell interactions and a marker of memory B cells; CD30+, a TNF receptor superfamily member that can mediate signal transduction events that can stimulate proliferation or initiate apoptotic cell death pathway; CD45+, a leukocyte marker that aids in regulating cell growth and differentiation; and CD138+, a plasma cell marker which aids in cell proliferation and migration⁸⁷. A brief discussion of the results of this study, for the various experiments, are given in the following sections.

Impact of KSHV Δ vIL-6 gene on human B cell markers in culture

The baseline picture of marker presence in the original B cells was provided by the initial phenotypic analysis of both KSHV WT cells and KSHV Δ vIL-6 cells within culture before injection into the mice. This uncovered patterns present within these cells before tumor growth. Higher GFP+, CD22+, and CD138+ expression was seen in cells without vIL-6. We can assume that these differences are due to the selection process made during the development of both of these virally-infected B cells.

Impact of vIL-6 on B cell makers in both KSHV Δ vIL-6 and KSHV WT-infected cells after tumor development

After excising the tumors, the profiles of the two cell groups were evaluated after tumor development. When comparing each group of cells before and after infection we see that, generally, expression decreases

in vivo vs. *in vitro* - except in the case of CD30⁺ cells, which increase. This trend of decreasing markers can be explained through the common phenomenon of cell de-differentiation throughout cancer development.

Cellular differentiation is the process whereby a cell changes from one cell type to another in order to specialize in a specific function⁸⁸. Conversely, de-differentiation is a phenomenon seen throughout the conversion of a normal cell into an oncogenic one. These cells become less specialized as they revert to an earlier developmental stage to survive. Two major nonexclusive hypotheses of the cellular origin of cancer are that malignancy arises from either stem cells experiencing maturation arrest or de-differentiation of mature cells that retain the ability to proliferate⁸⁹.

A common theme exhibited in both strains is the increase in CD30⁺ cells after tumorigenesis. A tumor necrosis factor, CD30 (or TNFRSF8) is a cell membrane protein found on activated T and B cells⁹⁰. Stimulation of CD30 has been shown to lead to proliferation as well as apoptotic death⁹¹. This information supports the selection of oncogenic cells amongst KSHV-infected B cells.

Impact of KSHV Δ vIL-6 gene on human B cell markers in cells extracted from tumors

When the expression profiles were compared between both KSHV WT and KSHV Δ vIL-6-infected cells, after tumor growth, there were several significant differences. KSHV WT-infected cells showed an increase in CD45⁺, but a decrease in live cells with GFP⁺ and CD30⁺ markers. This may be due to the selection process made during the construction of the KSHV-infected BJAB cells, as GFP⁺ cells were decreased in KSHV WT-infected cells compared with KSHV Δ vIL-6-infected cells before tumor growth. Cells containing vIL-6 express much less CD30 compared with those cells without vIL-6 after tumor growth, which may indicate that vIL-6 helps control CD30 expression. This would be advantageous to the virus in order to postpone detection as an oncogenic cell within the host. This, in turn, may allow for a

higher spread of the virus – which merits further investigation with an increased subject size to determine the significance in the difference in number of tumors developed between strains.

Summary

From this study we see various roles that vIL-6 could be playing within tumor development. One of these functions being that vIL-6 appears to increase the number, but not overall mass, of tumors. This indicates that vIL-6 increases the spread of cancer within the infected host, but not necessarily tumor growth. We also see that although CD30 increases *in vivo* compared to cultured cells, it appears that vIL-6 inhibits the frequency of CD30 relative to the mutant cells that did not contain vIL-6. Further investigation into how CD30 affects cancer development is needed before any conclusions can be made as to whether the vIL6 protein could potentially be used as a target for cancer treatment in the future.

Chapter 2

Results

While the initial study reported in the previous chapter focused on the presence and absence of the vIL-6 protein in the injected B cells, a second control experiment was undertaken using uninfected BJAB cells. This study compared the tumor progression with and without the KSHV virus. The expectation was that BJAB cells would not promote tumor development due to their lack of oncogenic viral infection. Preliminary findings suggested that this was not the case, so a more in-depth study was undertaken. This chapter presents the results of this investigation.

Tumor Analysis

As described in previous sections, tumors were harvested from Balb/c Rag2^{-/-} γ c^{-/-} mice 5 weeks after they were injected with 5×10^6 live cells from each group of cultured cells subcutaneously, directly over the abdomen. As for the experiment described in the previous chapter, the mass of each tumor was recorded, and the overall mass and number of tumors was analyzed.

In this particular case, there was no significant difference ($p=0.73$) between the number of tumors in BJAB-injected mice and WT-KSHV-injected mice (**Figure 10**); both cell types resulted in more tumors than the KSHV vIL-6 mutant virus. However, BJAB-injected mice exhibited tumors of significantly larger mass (**Figure 11**); the average tumor mass is more than double that of WT-injected mice, resulting in a statistical significance given by $p=0.040$.

Once again, the reasoning behind this difference in behavior for the two cell types is not immediately clear. Hence a more detailed study of the expression profiles was once again undertaken, as summarized in the next few sections. As before, cell markers associated with the following experiments are contrasted and compared.

1. Cells with and without KSHV grown in culture (uninfected BJAB vs KSHV WT-infected BJAB)
2. Uninfected BJAB cells before and after tumor development
3. KSHV WT-infected cells before and after tumor development
4. Cells with and without KSHV after tumor growth (uninfected BJAB vs KSHV WT-infected BJAB)

Comparison of expression profiles for uninfected immortalized BJAB cells and KSHV WT-infected BJAB cells in culture

Differences in gene expression patterns between our immortalized BJAB cell line and the BJAB construct containing KSHV were cataloged using flow cytometry. BJAB cell populations grown in culture were analyzed in order to determine any differences before infecting the mice with immortalized B cells with and without KSHV. We later performed similar experiments comparing cells extracted from tumors that developed inside of mice. The profiles taken of cultured cells were compared with those that were extracted from tumors in order to determine if changes in gene expression took place during the process of tumor development due to the presence of KSHV.

Most experiments were directed at B cell markers because our BJAB construct is a human B cell line. GFP expression (viral constructs contain the GFP gene) also allowed verification of a KSHV-infection within BJAB cells before the mice were injected (**Figure 4**).

Looking at the frequency of markers (**Figure 12A**) it can be seen that KSHV WT-infected BJAB cells displayed 8.83% more CD45+ ($p < 0.0001$) and 2.857% more CD45+CD20+ ($p = 0.0192$) expressing cells than uninfected immortalized B cells. KSHV -infected BJAB cells were also seen to downregulate CD45+CD22+ markers by 30.13% compared to uninfected BJAB cells ($p < 0.0001$).

As before, this dataset provided a baseline for comparison with the other experimental conditions, and indicated that certain genes were expressed differently in cells depending upon the presence or absence of KSHV. The cells were then re-analyzed to examine the mean fluorescence intensity (MFI) of different cell surface markers. MFI measures the intensity of antibody binding to cellular markers, and so in addition to determining if a gene was expressed or not (**Figure 10A**) we also examined if genes were expressed at different levels by measuring the MFI (**Figure 12B & Figure 6**).

Mean fluorescence intensity of these populations (**Figure 12**) showed a lower intensity in KSHV-infected BJAB cells compared with uninfected BJAB cells in CD45+CD19+ markers; CD45+CD22+ markers; and CD45+CD138+ markers. The differences being 1.7×10^4 lower CD45+CD19+ ($p=0.0342$), 5.1×10^3 lower CD45+CD22+ ($p < 0.0001$), and 1.2×10^3 lower CD45+CD138+ ($p=0.0180$) in KSHV-infected BJAB cells compared with uninfected BJAB cells.

Comparing expression profiles of immortalized BJAB cells grown in culture vs those extracted from tumors

Changes to the expression profiles of the immortalized B cells were explored following our preliminary tumor analysis, so as to explore anomalies made to the baseline documented in the previous section due to tumor growth.

Immortalized BJAB cultures showed increases in frequency (**Figure 13A**) of CD45+CD20+ markers by 23.41% ($p=0.0003$); CD45+CD22+ markers by 65.88% ($p < 0.0001$); and CD45+CD138+ markers by 12.28% ($p=0.0042$) compared with uninfected BJAB. BJAB cells found in the tumors of injected mice upregulated CD45+CD30+ markers 17.34% compared with BJAB cells grown in culture ($p=0.0059$). A trend of decreased cellular markers following tumor development is exhibited in most markers except that of CD30.

Mean fluorescence intensity of cultured BJAB cells (**Figure 13B**) showed higher intensities for CD45+ markers by 8.1×10^4 ($p < 0.0001$); CD45+CD19+ markers by 5.4×10^4 ($p < 0.0001$); CD45+CD20+ markers by 3.4×10^4 ($p < 0.0001$); CD45+CD22+ markers by 5.8×10^3 ($p < 0.0001$); and CD45+CD30+ markers by 1.4×10^4 ($p = 0.0315$) compared with BJAB tumors of injected mice. The results of the intensities shown establish the decrease of cellular markers, even in that of CD30.

Comparing expression profiles of KSHV WT-infected cells grown in culture vs those extracted from tumors

As mentioned in the previous chapter, deviations to the initial profiles of KSHV WT-infected BJAB cells as a result of tumor growth were also analyzed using flow cytometry. Cultured KSHV-infected cells contained higher frequencies (**Figure 7A**) of CD45 markers; CD45+GFP+ markers; CD45+CD19+ markers; CD45+CD20+ markers; CD45+CD22+ markers; and CD45+CD138+ markers compared with cells collected from tumors of KSHV-injected mice. CD45+ having a 12.40% decrease ($p < 0.0001$), CD45+GFP+ a 52.33% decrease ($p < 0.0001$), CD45+CD20+ a 27.41% decrease ($p = 0.0009$), CD45+CD22+ a 36.56% decrease ($p < 0.0001$), and CD45+CD138+ a 10.47% decrease ($p < 0.0001$) in tumor cells compared with cultured cells. CD45+CD30+ expression was upregulated in KSHV-infected tumor cells by 13.66% ($p < 0.0001$). There are a significant number of decreased markers following tumor growth in the case of KSHV WT-infected cells. CD45+CD30+ cells are shown to again increase.

Mean fluorescence intensity of cultured KSHV WT-infected cells (**Figure 7B**) showed higher intensities for CD45+ markers by 7.7×10^4 ($p < 0.0001$); CD45+GFP+ by 9.3×10^4 ($p < 0.0001$); CD45-GFP+ by 4.3×10^4 ($p = 0.0006$); CD45+CD19+ markers by 4.6×10^4 ($p < 0.0001$); CD45+CD20+ markers by 4.4×10^4 ($p < 0.0001$); CD45+CD22+ markers by 1.4×10^3 ($p < 0.0001$); and CD45+CD30+ markers by 1.6×10^4 ($p = 0.0127$) compared with KSHV-infected tumor cells. The MFI of most markers show a significant decrease in intensity when comparing cells post tumor-development vs. pre tumor-development.

Comparing expression profiles of uninfected BJAB cells and KSHV WT-infected BJAB cells extracted from tumors

Differences in the expression profiles of immortalized B cells and KSHV-infected B cells were again analyzed following the preliminary tumor analysis in order to expound on our findings. We hoped that a more in-depth explanation of our significant results could be garnered through FACS analysis.

When we looked at the frequencies of uninfected and KSHV-infected tumor cells (**Figure 14A**) we saw that KSHV-infected tumor cells downregulated live CD30+ markers by 9.057% *in vivo* compared to the uninfected BJAB infection ($p=0.0358$). This confirmed a higher number of CD30+ cells in uninfected BJAB tumors compared with KSHV-infected tumors.

Mean fluorescence intensity of these populations (**Figure 14B**) showed a lower intensity in KSHV-infected BJAB cells compared with uninfected BJAB cells in CD45+CD20+ markers and live CD30+ markers. The differences being 1.1×10^4 lower CD20 ($p=0.0271$), and 2.8×10^3 lower CD30 ($p=0.0037$). A discrepancy in CD30 markers between the two cell groups was confirmed by the lower intensity of binding in virally-infected cells.

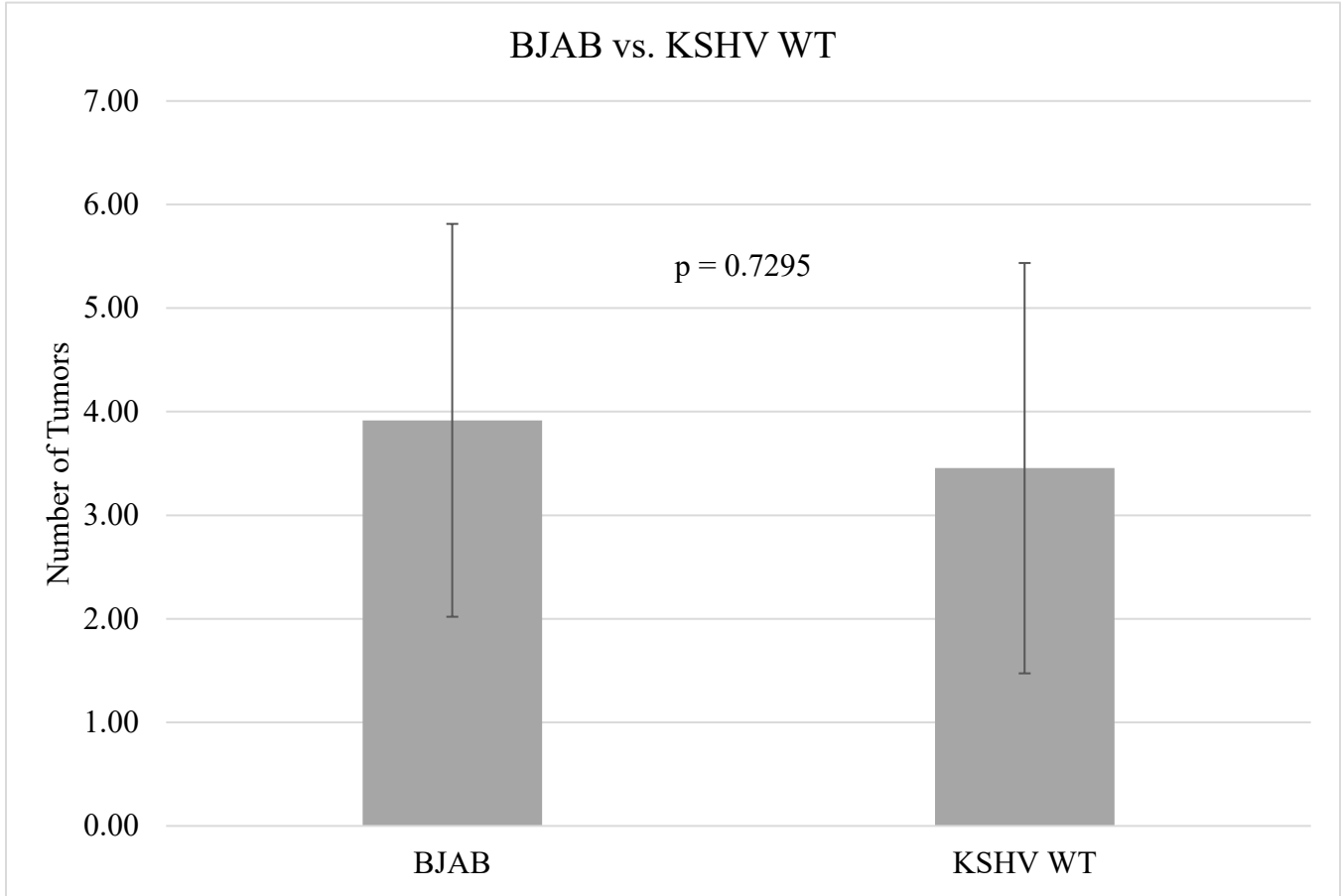


Figure 10. KSHV does not affect the number of tumors derived from injected mice. Each tumor was carefully excised from the mice and numbered at 5 weeks. The total number of tumors in each mouse from both groups was then analyzed. (n=12, n=11)

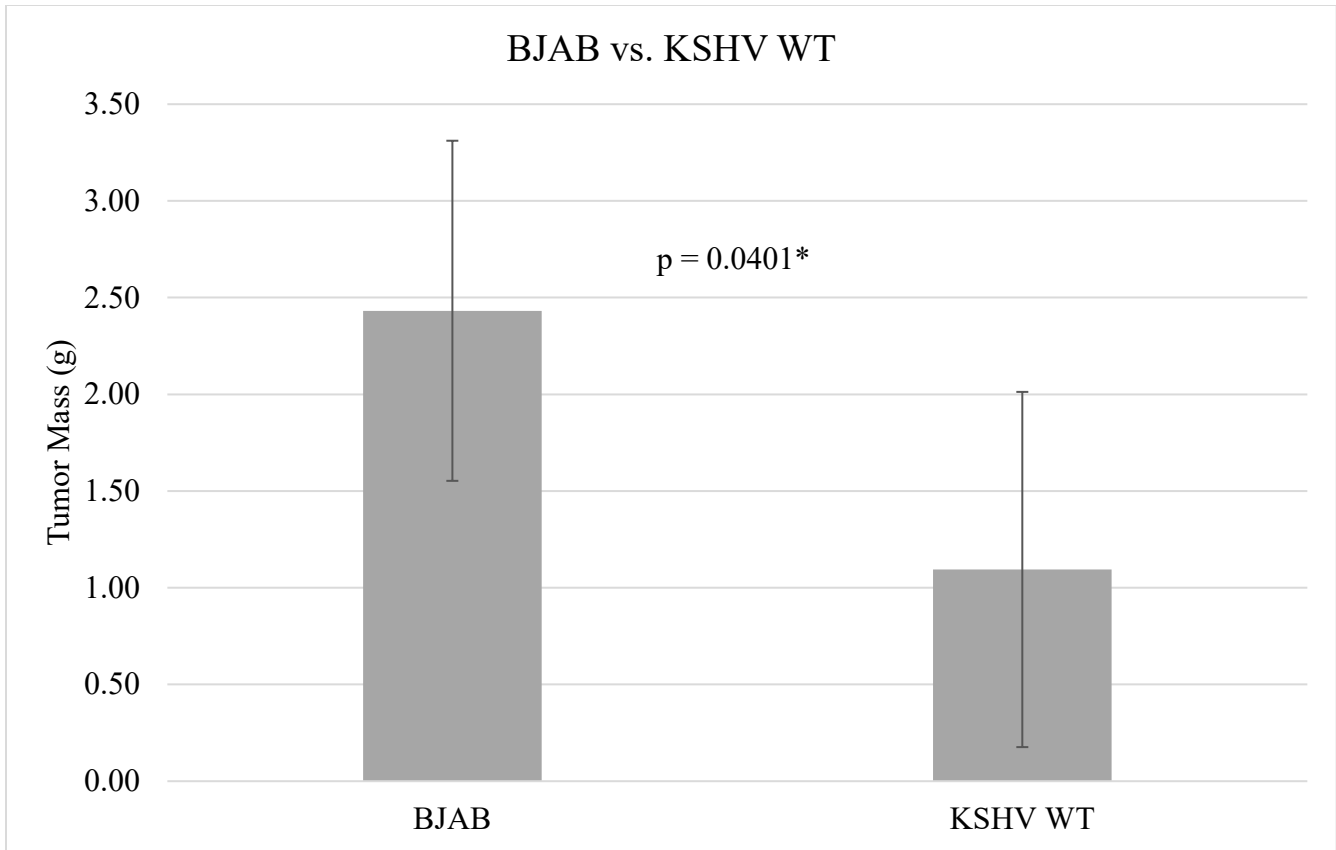


Figure 11. KSHV impacts mass of tumors in immortalized BJAB and KSHV WT-injected mice. Each tumor was carefully excised from the mice and weighed at 5 weeks. The total weight of each group was then analyzed. (* indicates a statistical significance less than $p = 0.05$ according to a pooled t-test analysis) (n=12, n=11)

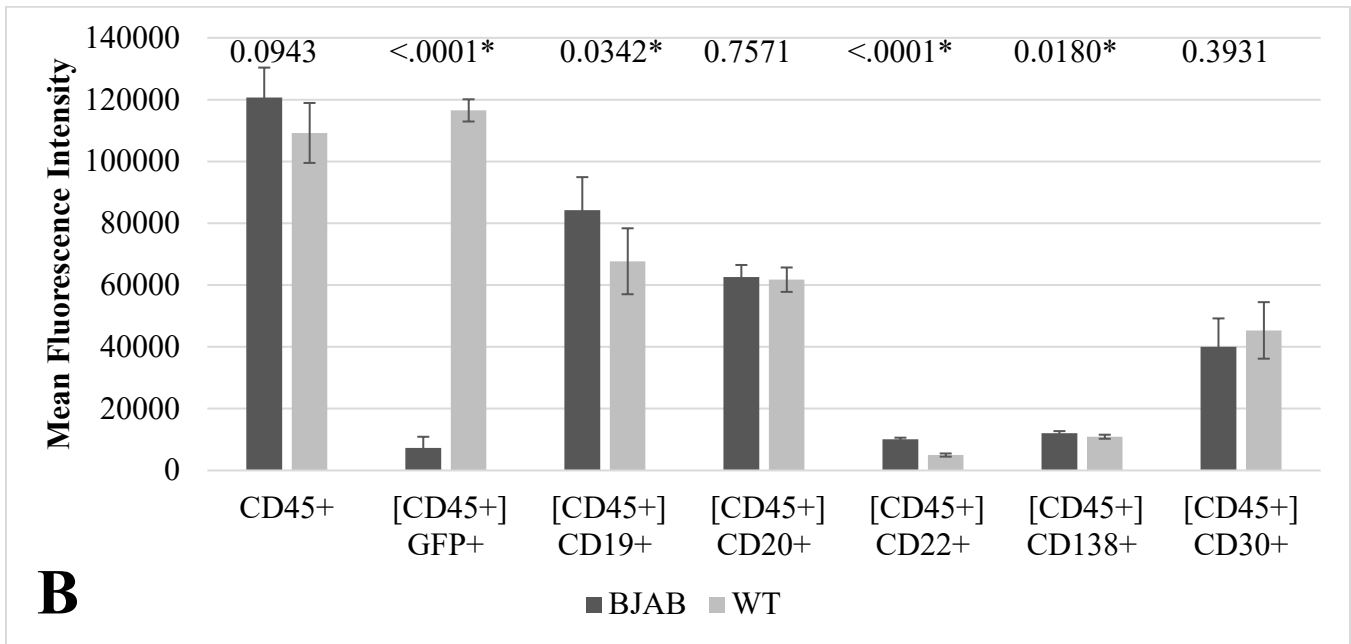
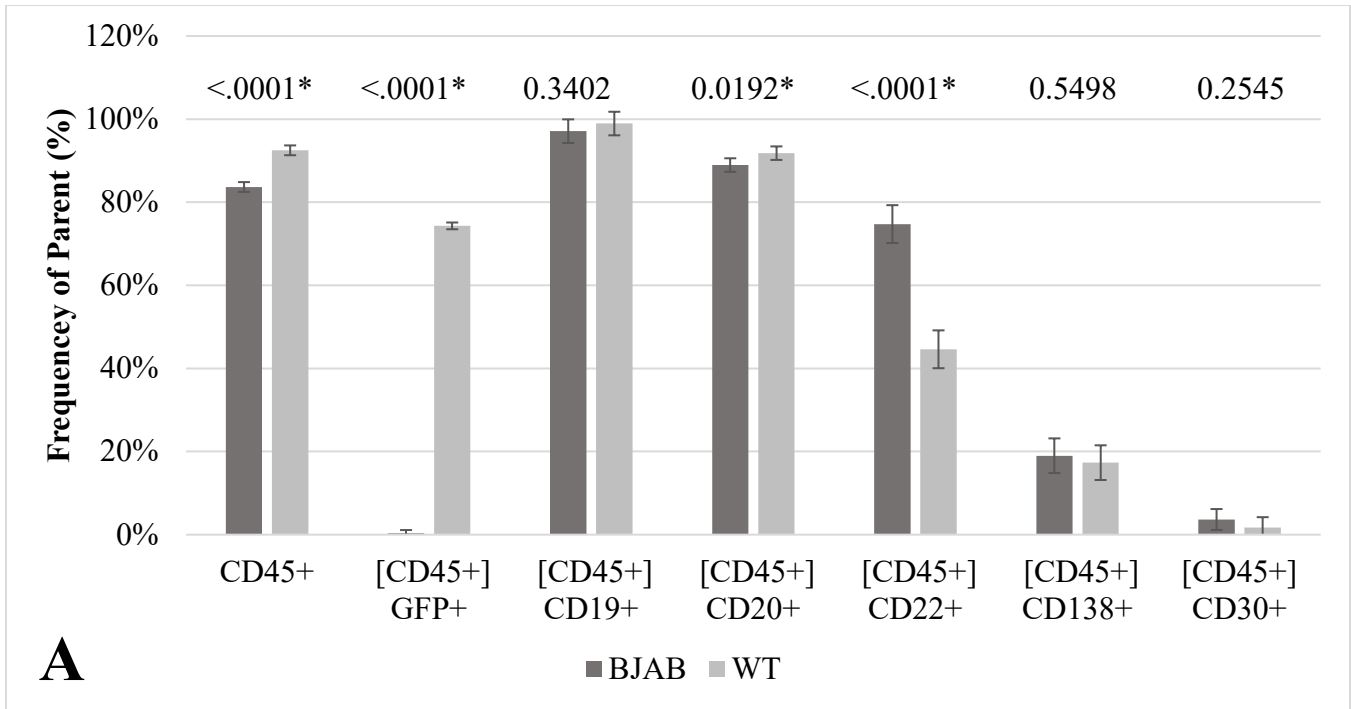


Figure 12. FACS analysis comparison of cultured immortalized BJAB and KSHV WT-injected BJAB cells. A, Frequency of CD45+ cells, which display markers for GFP, CD19, CD20, CD22, CD138, and CD30; B, Mean fluorescence intensity of CD45+ cells, which display markers for GFP, CD19, CD20, CD22, CD138, and CD30. (* indicates a statistical significance less than p = 0.05 according to a pooled t-test analysis)

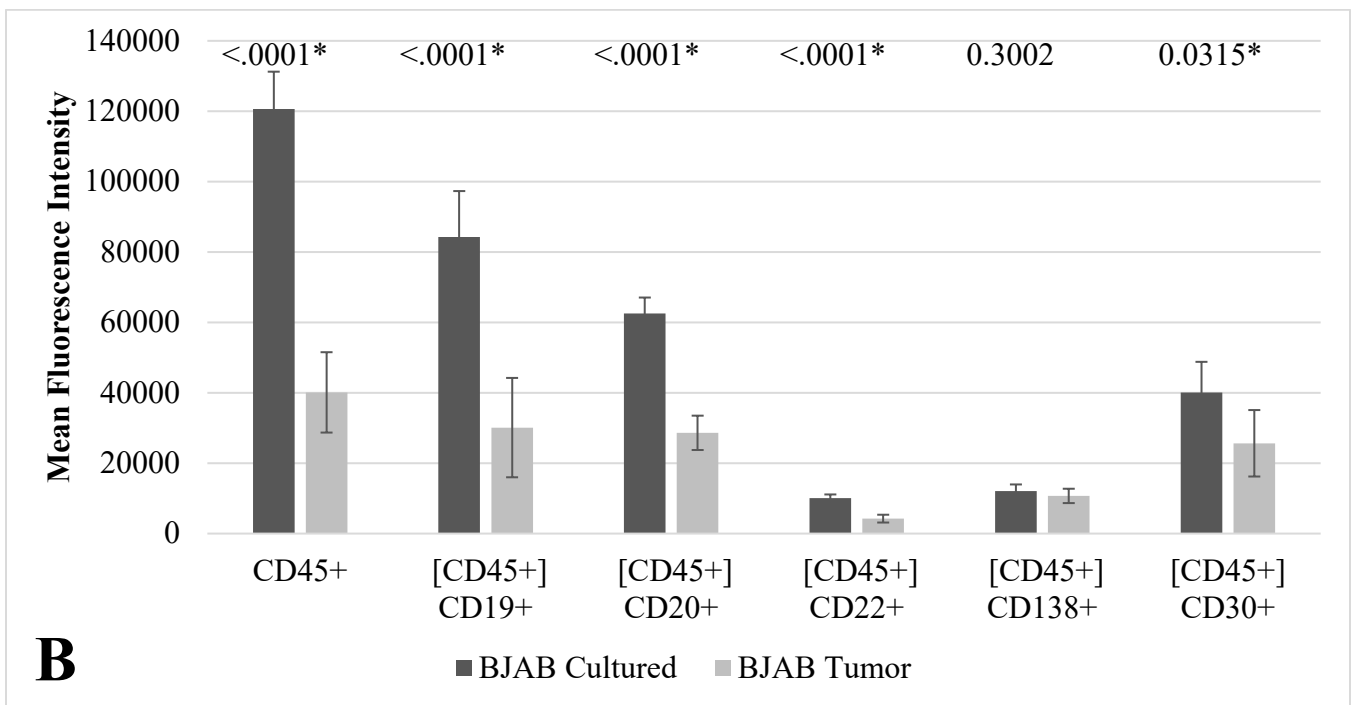
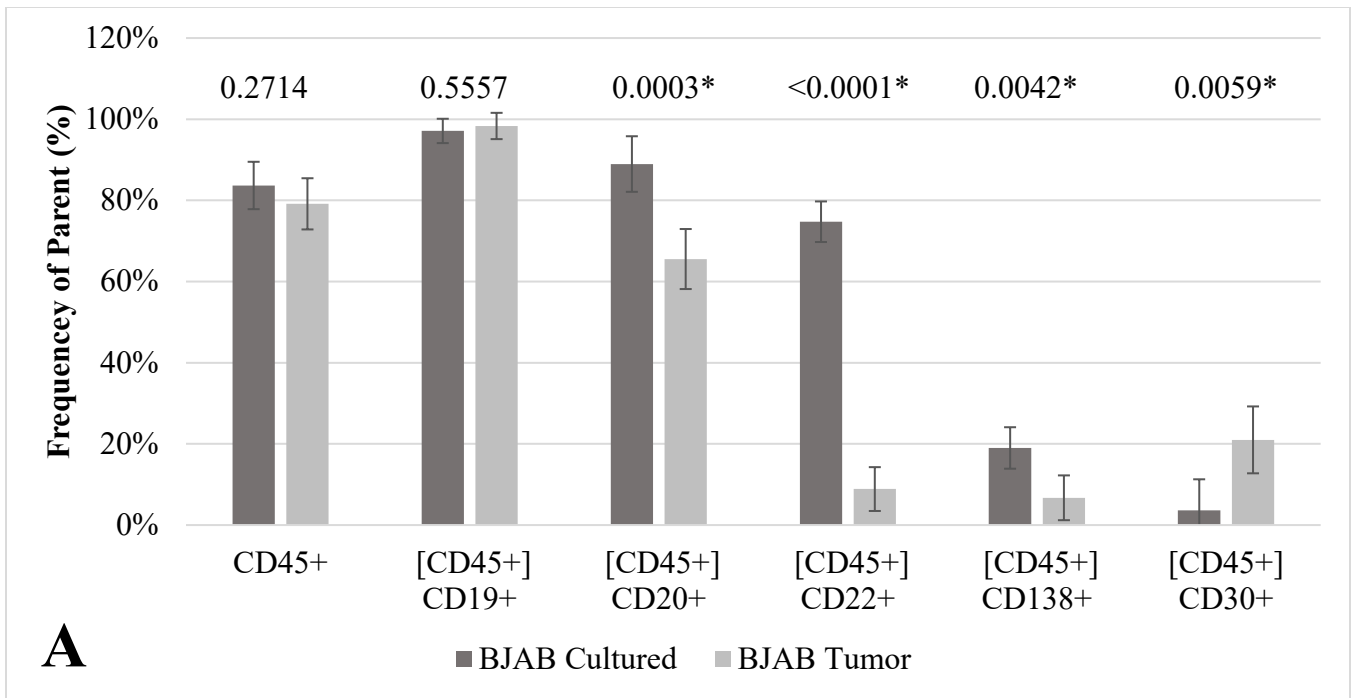


Figure 13. FACS analysis comparison of cultured immortalized BJAB cells and those extracted from tumors. *A*, Frequency of CD45+ cells, which display markers for GFP, CD19, CD20, CD22, CD138, and CD30; *B*, Mean fluorescence intensity of CD45+ cells, which display markers for GFP, CD19, CD20, CD22, CD138, and CD30. (* indicates a statistical significance less than p = 0.05 according to a pooled t-test analysis)

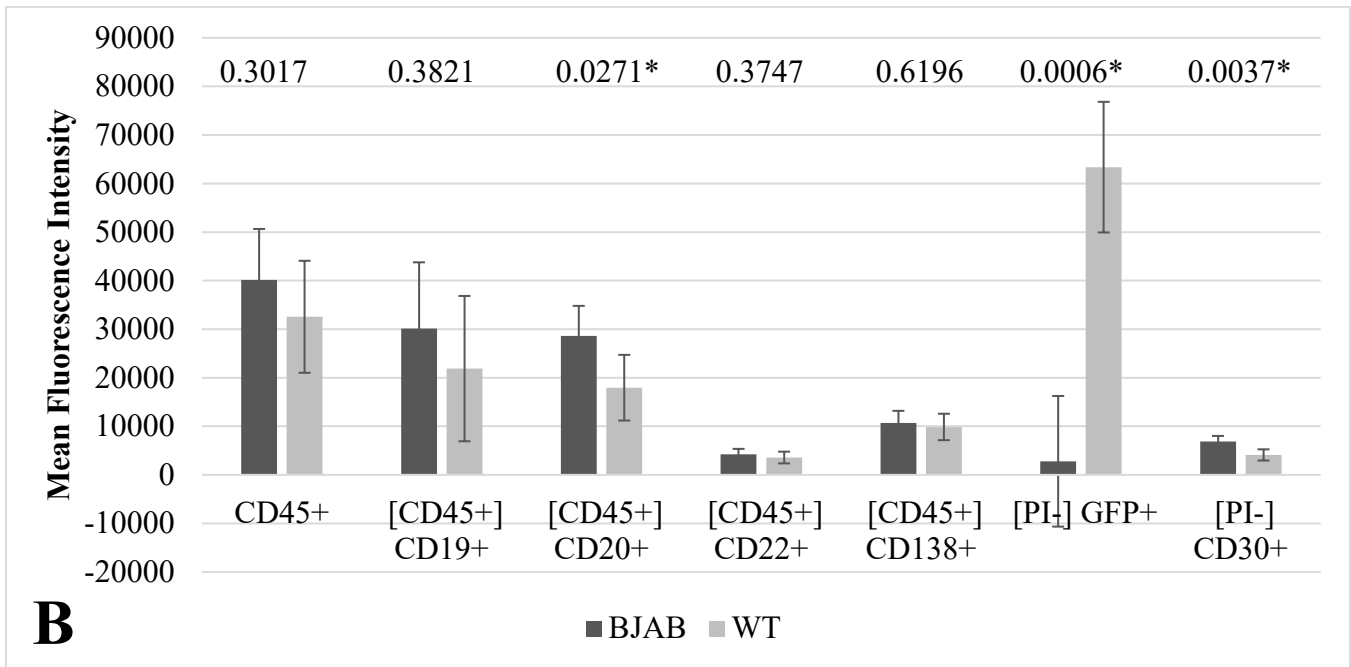
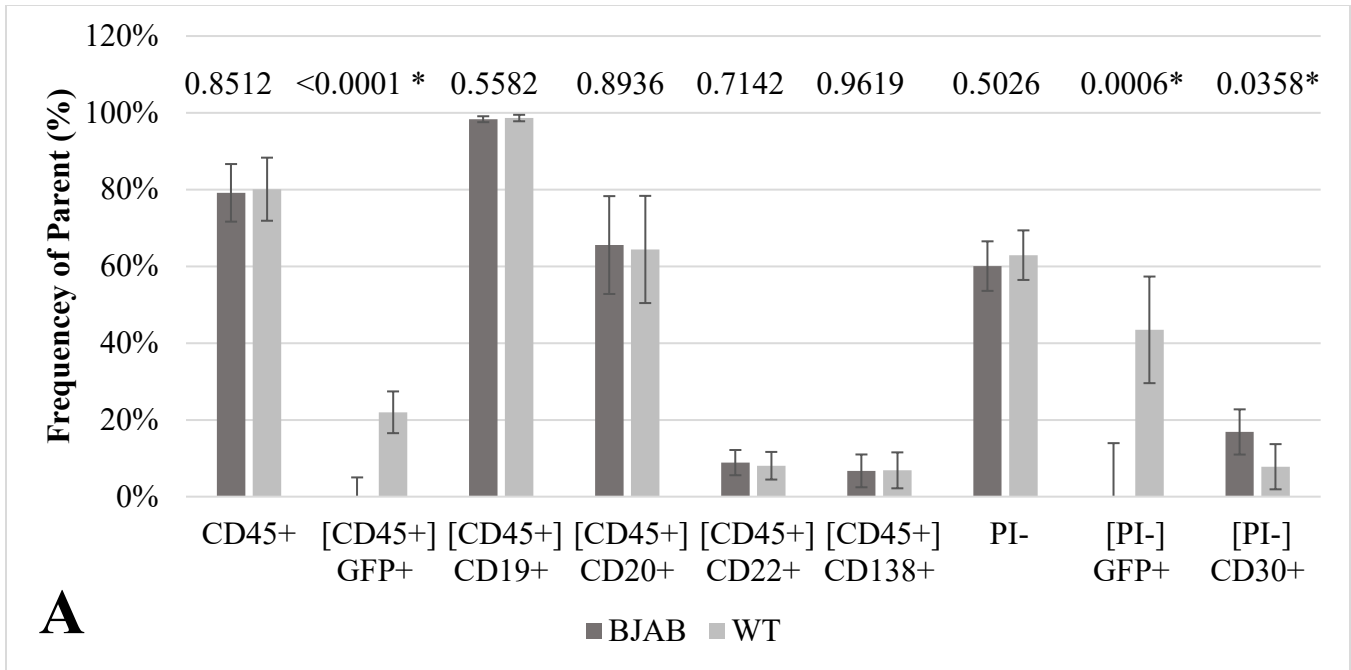


Figure 14. FACS analysis comparison of immortalized BJAB and KSHV WT-injected BJAB cells extracted from tumors. A, Frequency of CD45+ and propidium iodine-negative populations, which display markers for GFP, CD19, CD20, CD22, CD138, and CD30; B, Mean fluorescence intensity of CD45+ cells, which display markers for GFP, CD19, CD20, CD22, CD138, and CD30. (* indicates a statistical significance less than $p = 0.05$ according to a pooled t-test analysis)

Discussion

The initial hypothesis did not anticipate tumors from the secondary negative control, i.e. uninfected immortalized B cells (BJAB). It was expected that there would be a higher number of tumors and higher tumor mass in the wild-type KSHV injected mice compared with uninfected BJAB cells, considering KSHV is an oncogenic virus. This did not turn out to be the case.

Analysis of Tumors

There was no significant difference between the number of tumors in BJAB-injected mice and KSHV WT-injected mice. Both types resulted in an average number of tumors between 3 and 4. However, the size of the tumors was significantly different.

KSHV-infected cells produced smaller tumors than the oncogenic B cell line used in this experiment (BJAB). Not only was the size of tumors present with the oncogenic virus expected to be larger than that for the immortalized B cell line, but tumors themselves were not predicted for the immortalized cells.

It was hoped that the study of cell markers would shed more light on these results. The markers that were quantified included: CD19+, a B cell marker; CD20+, a B cell marker that aids in differentiation into plasma cells; CD22+, a regulatory molecule of B cell interactions; CD30+, a TNF receptor superfamily can mediate signal transduction events that can Stimulate Proliferation or initiate apoptotic cell death pathway; CD45+, a leukocyte marker that aids in regulating cell growth and differentiation; CD138+, a plasma cell marker which aids in cell proliferation and migration⁸⁷.

Impact of KSHV on human B cell markers in culture

A preliminary phenotypic analysis was performed for both KSHV WT-infected BJAB cells and uninfected BJAB cells within culture before injection into the mice. This allowed us to see any patterns within these cells before tumor-growth. WT-infected BJAB cells displayed a higher percentage of CD45+ and CD20+

markers in culture compared to BJAB cells. WT-infected BJAB cells were also seen to have lower CD22+ markers compared to negatively-infected BJAB cells. We can assume that these differences are due to the selection process made during the development of both of these virally-infected B cells.

Impact of KSHV on B cell makers in both infected and uninfected cells after tumor development

After excising the tumors we looked at the profiles of the two cell groups after tumor development. When comparing each group of cells before and after infection we see that, generally, expression decreases *in vivo* vs. *in vitro* - except in the case of CD30+ cells, which increase. This trend of decreasing markers can be explained through the common phenomenon of cell de-differentiation throughout cancer development.

Cellular differentiation is the process whereby a cell changes from one cell type to another in order to specialize in a specific function⁸⁸. Dedifferentiation, on the other hand, is a phenomenon seen throughout the conversion of a normal cell into an oncogenic one. These cells become less specialized as they revert to an earlier developmental stage to survive. Two major nonexclusive hypotheses of the cellular origin of cancer are that malignancy arises from either stem cells experiencing maturation arrest or dedifferentiation of mature cells that retain the ability to proliferate⁸⁹.

A common theme exhibited in both strains is the increase in CD30+ cells after tumorigenesis. A tumor necrosis factor, CD30 (or TNFRSF8) is a cell membrane protein found on activated T and B cells⁹⁰. Stimulation of CD30 has been shown to lead to proliferation as well as apoptotic death⁹¹. The anti-apoptotic effects of CD30 are mediated through the CD30-TRAF-NF- κ B pathway^{92,93}; the cytoplasmic tail of CD30 associating with TNF receptor-associated factors (TRAF) and activating NF- κ B transcription factors⁹⁴. Thus, we hypothesize that the increased CD30 levels in uninfected BJAB cells may cause an increase in anti-apoptotic genes, resulting in larger tumors.

Impact of KSHV on human B cell markers in cells extracted from tumors

When we compare the expression profiles of both BJAB cells and KSHV WT-infected BJAB cells, after tumor growth, we see a few differences. This may be merely due to the selection process made during the construction of the KSHV-infected BJAB cells and other lineage-selection processes, as they display the same patterns both before and after infection. We do notice that CD30 remains an irregularity, of which we see that those cells containing KSHV express much less CD30 compared with those cells without the virus. This may indicate that KSHV has a method of controlling CD30 expression; this may allow virally-infected cancerous cells to survive longer within the host undetected, it may be possible that smaller tumors indicate increased viability of the virus within the tumor, or potentially, the virus is trying not to kill the host as quickly as it might if it developed larger tumors.

Summary

The lack of significant change in overall tumor mass, and the marginally significant increase in tumor numbers associated with vIL-6 described in the previous chapter led to the further studies to compare uninfected cells with those containing KSHV. Smaller massed tumors were seen in those oncogenic cells infected with wild-type KSHV compared to uninfected immortalized B cells, although no difference in the number of tumors was observed. This indicates that the virus somehow slows tumor development. Lower levels of CD30⁺ cells were also seen in cells infected with wild-type KSHV compared to uninfected immortalized B cells. This may play a role in the differences in tumor development that we see between the different cell groups, as CD30 could be aiding in a lack of apoptosis in immortalized B cells. More studies must be done in order to evaluate how this could be advantage for the virus.

Conclusion

Our initial hypothesis was that viral interleukin-6 is necessary for tumor development in larger tumors such as those found in MCD; therefore, when present, it is expected to increase tumor mass and promote angiogenesis as well as metastasis of the tumor. After preliminary data was acquired, we focused on two different areas of KSHV oncogenesis: the role of vIL-6 in KSHV-associated cancers, and the implications of a KSHV infection on the immortalized cell-line, BJAB. By obtaining a strain of KSHV with a vIL-6 knockout, we were able to investigate the role of the virally-produced cytokine. Based upon the subsequent cancer growth in twelve mice, the results indicated no significant change in overall tumor mass, but an appreciably higher number of tumors relating to the presence of vIL-6. While the statistical significance of the higher number of tumors was below the 95th percentile t-test, it is likely that a higher subject number would produce a clear statistical significance; this would indicate that vIL-6 increases the number of tumors compared with the vIL-6 knockout strain. The various mechanisms associated with the presence of the protein may allow the virus to increase the spread of cancer within an injected host, even though the tumors do not increase in mass. Along with this preliminary tumor analysis, the cell-surface phenotype was analyzed. Examination of these variables showed that CD30 markers increased in frequency within *in vivo* cells compared to cultured cells; however, vIL-6 seemed to inhibit the increase of CD30 relative to the mutant cells that did not contain vIL-6. In order to fully understand how this relationship affects viral oncogenesis, further investigation into the role of CD30 in KSHV infections is needed. This would also allow for the increased understanding necessary to make final conclusions as to whether the vIL6 protein could be used as a target for cancer treatment in the future.

A second course of study was then undertaken to further understand how a KSHV-infection could affect immortalized cells transplanted into an immunocompromised murine host. Initial tumor analysis indicated tumors with lower mass in KSHV-infected cells compared to uninfected immortalized B cells. This was

interesting as it indicates that the viral-infection of a known oncogenic virus decreases tumor development. Further investigation with expression profiles was performed for a more complete study. This showed lower levels of CD30+ cells were present in KSHV-infected cells compared to the uninfected immortalized B cells. If CD30 is considered to be playing a role in anti-apoptotic gene expression in this type of oncogenesis, this could explain the differences in tumor mass that we see between the two cell groups. The question then follows; why would an oncogenic virus be avoiding anti-apoptotic gene expression? More studies must be done in order to evaluate how this could be advantage for the virus, and what exact mechanisms of CD30 are being use in these types of cancers.

References

1. Mukherjee, S. *The Emperor of All Maladies: A Biography of Cancer: Siddhartha Mukherjee: 9781439170915: Amazon.com: Books.* (A Division of Simon and Schuster, Inc., 2010).
2. National Center for Health Statistics. *Health, United States, 2015.* (2016). at <<http://www.cdc.gov/nchs/data/hus/hus15.pdf#019>>
3. National Cancer Institute. *Defining Cancer.* (2014). at <<https://www.cancer.gov/about-cancer/understanding/what-is-cancer>>
4. Stewart, B. W., Wild, C., International Agency for Research on Cancer. & World Health Organization. *World cancer report 2014.* (International Agency for Research on Cancer, 2014).
5. Aresté, C. & Blackbourn, D. J. Modulation of the immune system by Kaposi's sarcoma-associated herpesvirus. *Trends Microbiol.* **17**, 119–129 (2009).
6. Kaposi, M. Idiopathisches multiples Pigmentsarkom der Haut. *Arch Dermatol Syph* 265–273 (1872).
7. Alberts, B. *et al. Molecular Biology of the Cell. 4th edition: The Generation of Antibody Diversity.* (Garland Science, 2002). at <<http://www.ncbi.nlm.nih.gov/books/NBK26860/>>
8. Beral, V., Peterman, T. A., Berkelman, R. L. & Jaffe, H. W. Kaposi's sarcoma among persons with AIDS: a sexually transmitted infection? *Lancet* **335**, 123–128 (1990).
9. Beral, V., Peterman, T. A., Berkelman, R. L. & Jaffe, H. W. Kaposi's sarcoma among persons with AIDS: a sexually transmitted infection? *Lancet* **335**, 123–128 (1990).
10. Chang, Y. *et al.* Identification of herpesvirus-like DNA sequences in AIDS-associated Kaposi's sarcoma. *Science* **266**, 1865–9 (1994).

11. Gramolelli, S. & Schulz, T. F. The role of Kaposi sarcoma-associated herpesvirus in the pathogenesis of Kaposi sarcoma. *J. Pathol.* **235**, 368–380 (2015).
12. Brown, J. C. & Newcomb, W. W. Herpesvirus capsid assembly: insights from structural analysis. *Curr. Opin. Virol.* **1**, 142–9 (2011).
13. Bechtel, J. T., Winant, R. C. & Ganem, D. Host and viral proteins in the virion of Kaposi's sarcoma-associated herpesvirus. *J. Virol.* **79**, 4952–64 (2005).
14. Zhu, F. X., Chong, J. M., Wu, L. & Yuan, Y. Virion proteins of Kaposi's sarcoma-associated herpesvirus. *J. Virol.* **79**, 800–11 (2005).
15. Cattani, P. *et al.* Human herpesvirus 8 seroprevalence and evaluation of nonsexual transmission routes by detection of DNA in clinical specimens from human immunodeficiency virus-seronegative patients from central and southern Italy, with and without Kaposi's sarcoma. *J. Clin. Microbiol.* **37**, 1150–3 (1999).
16. de França, T. R. T., de Araújo, R. A., Ribeiro, C. M. B. & Leao, J. C. Salivary shedding of HHV-8 in people infected or not by human immunodeficiency virus 1. *J. Oral Pathol. Med.* **40**, 97–102 (2011).
17. Hladik, W. *et al.* Transmission of human herpesvirus 8 by blood transfusion. *N. Engl. J. Med.* **355**, 1331–8 (2006).
18. Francès, C. *et al.* The impact of preexisting or acquired Kaposi sarcoma herpesvirus infection in kidney transplant recipients on morbidity and survival. *Am. J. Transplant* **9**, 2580–6 (2009).
19. de Sanjose, S. *et al.* Geographic variation in the prevalence of Kaposi sarcoma-associated herpesvirus and risk factors for transmission. *J. Infect. Dis.* **199**, 1449–56 (2009).
20. Kedes, D. H. *et al.* The seroepidemiology of human herpesvirus 8 (Kaposi's sarcoma-associated

- herpesvirus): distribution of infection in KS risk groups and evidence for sexual transmission. *Nat. Med.* **2**, 918–24 (1996).
21. Lukac, D. M., Kirshner, J. R. & Ganem, D. Transcriptional activation by the product of open reading frame 50 of Kaposi's sarcoma-associated herpesvirus is required for lytic viral reactivation in B cells. *J. Virol.* **73**, 9348–61 (1999).
 22. Hu, J., Garber, A. C. & Renne, R. The latency-associated nuclear antigen of Kaposi's sarcoma-associated herpesvirus supports latent DNA replication in dividing cells. *J. Virol.* **76**, 11677–87 (2002).
 23. Cotter, M. A. & Robertson, E. S. The latency-associated nuclear antigen tethers the Kaposi's sarcoma-associated herpesvirus genome to host chromosomes in body cavity-based lymphoma cells. *Virology* **264**, 254–64 (1999).
 24. Kalt, I., Masa, S.-R. & Sarid, R. Linking the Kaposi's sarcoma-associated herpesvirus (KSHV/HHV-8) to human malignancies. *Methods Mol. Biol.* **471**, 387–407 (2009).
 25. Ballestas, M. E., Chatis, P. A. & Kaye, K. M. Efficient persistence of extrachromosomal KSHV DNA mediated by latency-associated nuclear antigen. **284**, 641–644 (1999).
 26. Ganem, D. KSHV INFECTION AND THE PATHOGENESIS OF KAPOSI'S SARCOMA. *Annu. Rev. Pathol. Mech. Dis.* **1**, 273–296 (2006).
 27. Sun, R. *et al.* A viral gene that activates lytic cycle expression of Kaposi's sarcoma-associated herpesvirus. *Proc. Natl. Acad. Sci. U. S. A.* **95**, 10866–71 (1998).
 28. Weber, K. S. *et al.* Selective recruitment of Th2-type cells and evasion from a cytotoxic immune response mediated by viral macrophage inhibitory protein-II. *Eur. J. Immunol.* **31**, 2458–66 (2001).
 29. Wen, K. W. & Damania, B. Kaposi sarcoma-associated herpesvirus (KSHV): molecular biology

- and oncogenesis. *Cancer Lett.* **289**, 140–50 (2010).
30. Cesarman, E., Chang, Y., Moore, P. S., Said, J. W. & Knowles, D. M. Kaposi's sarcoma-associated herpesvirus-like DNA sequences in AIDS-related body-cavity-based lymphomas. *N. Engl. J. Med.* **332**, 1186–91 (1995).
 31. Gessain, A. *et al.* Kaposi sarcoma-associated herpes-like virus (human herpesvirus type 8) DNA sequences in multicentric Castleman's disease: is there any relevant association in non-human immunodeficiency virus-infected patients? *Blood* **87**, 414–6 (1996).
 32. Soulier, J. *et al.* Kaposi's sarcoma-associated herpesvirus-like DNA sequences in multicentric Castleman's disease. *Blood* **86**, 1276–80 (1995).
 33. Franceschi, S. & Serraino, D. Kaposi's sarcoma and KSHV. *Lancet (London, England)* **346**, 1360–1 (1995).
 34. Boshoff, C. *et al.* Angiogenic and HIV-inhibitory functions of KSHV-encoded chemokines. *Science* **278**, 290–4 (1997).
 35. Coen, N., Duraffour, S., Snoeck, R. & Andrei, G. KSHV Targeted Therapy: An Update on Inhibitors of Viral Lytic Replication. *Viruses* **6**, 4731–4759 (2014).
 36. Wabinga, H. R., Parkin, D. M., Wabwire-Mangen, F. & Mugerwa, J. W. Cancer in Kampala, Uganda, in 1989-91: changes in incidence in the era of AIDS. *Int. J. cancer* **54**, 26–36 (1993).
 37. Ziegler, J. L. & Katongole-Mbidde, E. Kaposi's sarcoma in childhood: An analysis of 100 cases from Uganda and relationship to HIV infection. *Int. J. Cancer* **65**, 200–203 (1996).
 38. Dourmishev, L. A., Dourmishev, A. L., Palmeri, D., Schwartz, R. A. & Lukac, D. M. Molecular genetics of Kaposi's sarcoma-associated herpesvirus (human herpesvirus-8) epidemiology and pathogenesis. *Microbiol. Mol. Biol. Rev.* **67**, 175–212, table of contents (2003).

39. Regamey, N. *et al.* Transmission of human herpesvirus 8 infection from renal-transplant donors to recipients. *N. Engl. J. Med.* **339**, 1358–63 (1998).
40. Siegel, J. H. *et al.* Disseminated visceral Kaposi's sarcoma. Appearance after human renal homograft operation. *JAMA* **207**, 1493–6 (1969).
41. Tamburro, K. M. *et al.* Vironome of Kaposi sarcoma associated herpesvirus-inflammatory cytokine syndrome in an AIDS patient reveals co-infection of human herpesvirus 8 and human herpesvirus 6A. *Virology* **433**, 220–5 (2012).
42. Dupin, N. *et al.* Distribution of human herpesvirus-8 latently infected cells in Kaposi's sarcoma, multicentric Castleman's disease, and primary effusion lymphoma. *Proc. Natl. Acad. Sci. U. S. A.* **96**, 4546–51 (1999).
43. Carbone, A. & Gloghini, A. KSHV/HHV8-associated lymphomas. *Br. J. Haematol.* **140**, 13–24 (2008).
44. Carbone, A. *et al.* Kaposi's sarcoma-associated herpesvirus/human herpesvirus type 8-positive solid lymphomas: a tissue-based variant of primary effusion lymphoma. *J. Mol. Diagn.* **7**, 17–27 (2005).
45. Boulanger, M. J. *et al.* Molecular Mechanisms for Viral Mimicry of a Human Cytokine: Activation of gp130 by HHV-8 Interleukin-6. *J. Mol. Biol.* **335**, 641–654 (2004).
46. Renne, R., Lagunoff, M., Zhong, W. & Ganem, D. The size and conformation of Kaposi's sarcoma-associated herpesvirus (human herpesvirus 8) DNA in infected cells and virions. *J. Virol.* **70**, 8151–4 (1996).
47. Gasperini, P., Sakakibara, S. & Tosata, G. Contribution of cell and viral cytokines to KSHV pathogenesis.pdf. *J. Leukoc. Biol.* **84**, 994–1000 (2008).

48. Gaidano, G. *et al.* Establishment of AIDS-related lymphoma cell lines from lymphomatous effusions. *Leukemia* **10**, 1237–40 (1996).
49. Chadburn, A. *et al.* Immunophenotypic analysis of the Kaposi sarcoma herpesvirus (KSHV; HHV-8)-infected B cells in HIV+ multicentric Castleman disease (MCD). *Histopathology* **53**, 513–24 (2008).
50. Polizzotto, M. N., Uldrick, T. S., Hu, D. & Yarchoan, R. Clinical Manifestations of Kaposi Sarcoma Herpesvirus Lytic Activation: Multicentric Castleman Disease (KSHV-MCD) and the KSHV Inflammatory Cytokine Syndrome. *Front. Microbiol.* **3**, 73 (2012).
51. Parravicini, C. *et al.* Expression of a virus-derived cytokine, KSHV vIL-6, in HIV-seronegative Castleman's disease. *Am. J. Pathol.* **151**, 1517–22 (1997).
52. Carbone, A., Cesarman, E., Spina, M., Gloghini, A. & Schulz, T. F. HIV-associated lymphomas and gamma-herpesviruses. *Blood* **113**, 1213–1224 (2009).
53. Oksenhendler, E. *et al.* High incidence of Kaposi sarcoma-associated herpesvirus-related non-Hodgkin lymphoma in patients with HIV infection and multicentric Castleman disease. *Blood* **99**, 2331–6 (2002).
54. Oksenhendler, E. *et al.* Multicentric Castleman's disease in HIV infection: a clinical and pathological study of 20 patients. *AIDS* **10**, 61–7 (1996).
55. Nishi, J. *et al.* Expression of vascular endothelial growth factor in sera and lymph nodes of the plasma cell type of Castleman's disease. *Br. J. Haematol.* **104**, 482–5 (1999).
56. Nishimoto, N. *et al.* Humanized anti-interleukin-6 receptor antibody treatment of multicentric Castleman disease. *Blood* **106**, 2627–32 (2005).
57. Oksenhendler, E. *et al.* High levels of human herpesvirus 8 viral load, human interleukin-6,

- interleukin-10, and C reactive protein correlate with exacerbation of multicentric castleman disease in HIV-infected patients. *Blood* **96**, 2069–73 (2000).
58. Yoshizaki, K. *et al.* Pathogenic significance of interleukin-6 (IL-6/BSF-2) in Castleman's disease. *Blood* **74**, 1360–7 (1989).
 59. Aoki, Y., Yarchoan, R., Braun, J., Iwamoto, A. & Tosato, G. Viral and cellular cytokines in AIDS-related malignant lymphomatous effusions. *Blood* **96**, 1599–601 (2000).
 60. Aoki, Y. Detection of viral interleukin-6 in Kaposi sarcoma-associated herpesvirus-linked disorders. *Blood* **97**, 2173–2176 (2001).
 61. Moore, P. S., Boshoff, C., Weiss, R. A. & Chang, Y. Molecular mimicry of human cytokine and cytokine response pathway genes by KSHV. *Science* **274**, 1739–44 (1996).
 62. Neipel, F. *et al.* Human herpesvirus 8 encodes a homolog of interleukin-6. *J. Virol.* **71**, 839–42 (1997).
 63. Nicholas, J. *et al.* Kaposi's sarcoma-associated human herpesvirus-8 encodes homologues of macrophage inflammatory protein-1 and interleukin-6. *Nat. Med.* **3**, 287–92 (1997).
 64. Pedersen, B. K. & Febbraio, M. A. Muscle as an endocrine organ: focus on muscle-derived interleukin-6. *Physiol. Rev.* **88**, 1379–406 (2008).
 65. Liang, C., Lee, J.-S. & Jung, J. U. Immune evasion in Kaposi's sarcoma-associated herpes virus associated oncogenesis. *Semin. Cancer Biol.* **18**, 423–436 (2008).
 66. Wijdenes, J. *et al.* Responses IL-6 Antagonistic Activity of Soluble gp130 on Soluble IL-6 Receptor Potentiates the Soluble IL-6 Receptor Potentiates the Antagonistic Activity of Soluble gp130 on IL-6 Responses. *J Immunol Ref.* **161116347**, 6347–6355 (1998).
 67. Aoki, Y. Receptor engagement by viral interleukin-6 encoded by Kaposi sarcoma-associated

- herpesvirus. *Blood* **98**, 3042–3049 (2001).
68. Chow, D., He, X., Snow, A. L., Rose-John, S. & Garcia, K. C. Structure of an extracellular gp130 cytokine receptor signaling complex. *Science* **291**, 2150–5 (2001).
69. Wan, X., Wang, H. & Nicholas, J. Human herpesvirus 8 interleukin-6 (vIL-6) signals through gp130 but has structural and receptor-binding properties distinct from those of human IL-6. *J. Virol.* **73**, 8268–78 (1999).
70. Hu, F. & Nicholas, J. Signal transduction by human herpesvirus 8 viral interleukin-6 (vIL-6) is modulated by the nonsignaling gp80 subunit of the IL-6 receptor complex and is distinct from signaling induced by human IL-6. *J. Virol.* **80**, 10874–8 (2006).
71. Li, H., Wang, H. & Nicholas, J. Detection of direct binding of human herpesvirus 8-encoded interleukin-6 (vIL-6) to both gp130 and IL-6 receptor (IL-6R) and identification of amino acid residues of vIL-6 important for IL-6R-dependent and -independent signaling. *J. Virol.* **75**, 3325–34 (2001).
72. Chen, D., Sandford, G. & Nicholas, J. Intracellular signaling mechanisms and activities of human herpesvirus 8 interleukin-6. *J. Virol.* **83**, 722–33 (2009).
73. Meads, M. B. & Medveczky, P. G. Kaposi's sarcoma-associated herpesvirus-encoded viral interleukin-6 is secreted and modified differently than human interleukin-6: evidence for a unique autocrine signaling mechanism. *J. Biol. Chem.* **279**, 51793–803 (2004).
74. Meads, M. B. & Medveczky, P. G. Kaposi's sarcoma-associated herpesvirus-encoded viral interleukin-6 is secreted and modified differently than human interleukin-6: evidence for a unique autocrine signaling mechanism. *J. Biol. Chem.* **279**, 51793–803 (2004).
75. Nicholas, J. *et al.* Novel organizational features, captured cellular genes, and strain variability

within the genome of KSHV/HHV8. *J. Natl. Cancer Inst. Monogr.* 79–88 (1998). at <<http://www.ncbi.nlm.nih.gov/pubmed/9709308>>

76. Mori, Y. *et al.* Human herpesvirus 8-encoded interleukin-6 homologue (viral IL-6) induces endogenous human IL-6 secretion. *J. Med. Virol.* **61**, 332–5 (2000).
77. Suthaus, J. *et al.* HHV-8-encoded viral IL-6 collaborates with mouse IL-6 in the development of multicentric Castleman disease in mice. *Blood* **119**, 5173–81 (2012).
78. Hideshima, T. *et al.* Characterization of Signaling Cascades Triggered by Human Interleukin-6 versus Kaposi's Sarcoma-associated Herpes Virus-encoded Viral Interleukin 6. *Clin. Cancer Res.* **6**, 1180–1189 (2000).
79. Giffin, L. & Damania, B. KSHV: pathways to tumorigenesis and persistent infection. *Adv. Virus Res.* **88**, 111–59 (2014).
80. Picchio, G. R. *et al.* The KSHV/HHV8-infected BCBL-1 lymphoma line causes tumors in SCID mice but fails to transmit virus to a human peripheral blood mononuclear cell graft. *Virology* **238**, 22–9 (1997).
81. Aoki, Y. *et al.* Angiogenesis and hematopoiesis induced by Kaposi's sarcoma-associated herpesvirus-encoded interleukin-6. *Blood* **93**, 4034–43 (1999).
82. Qian, L.-W., Xie, J., Ye, F. & Gao, S.-J. Kaposi's sarcoma-associated herpesvirus infection promotes invasion of primary human umbilical vein endothelial cells by inducing matrix metalloproteinases. *J. Virol.* **81**, 7001–10 (2007).
83. Molden, J., Chang, Y., You, Y., Moore, P. S. & Goldsmith, M. A. A Kaposi's Sarcoma-associated Herpesvirus-encoded Cytokine Homolog (vIL-6) Activates Signaling through the Shared gp130 Receptor Subunit. *J. Biol. Chem.* **272**, 19625–19631 (1997).

84. Chen, L. & Lagunoff, M. Establishment and maintenance of Kaposi's sarcoma-associated herpesvirus latency in B cells. *J. Virol.* **79**, 14383–91 (2005).
85. Chen, L. & Lagunoff, M. The KSHV viral interleukin-6 is not essential for latency or lytic replication in BJAB cells. *Virology* **359**, 425–35 (2007).
86. Davies, P. C. *et al.* Cancer as a dynamical phase transition. *Theor. Biol. Med. Model.* **8**, 30 (2011).
87. BD Biosciences. *CD Marker Handbook Human Mouse.* (2010). at https://www.bdbiosciences.com/documents/cd_marker_handbook.pdf
88. O'Conner, C. M. & Adams, J. U. *Essentials of Cell Biology.* (NPG Education, 2010). at <http://www.nature.com/scitable/ebooks/essentials-of-cell-biology-14749010>
89. Sell, S. Cellular Origin of Cancer: Dedifferentiation or Stem Cell Maturation Arrest? *Environ. Health Perspect.* **101**, 15 (1993).
90. O'Leary, N. *et al.* Reference sequence (RefSeq) database at NCBI: current status, taxonomic expansion, and functional annotation. Gene ID:943. *Nucleic Acids Res.* **44**, D733–45 (2016).
91. Baker, S. J. & Reddy, E. P. Transducers of life and death: TNF receptor superfamily and associated proteins. *Oncogene* **12**, 1–9 (1996).
92. Nishikori, M., Ohno, H., Haga, H. & Uchiyama, T. Stimulation of CD30 in anaplastic large cell lymphoma leads to production of nuclear factor-kappaB p52, which is associated with hyperphosphorylated Bcl-3. *Cancer Sci.* **96**, 487–497 (2005).
93. Turco, M. C. *et al.* NF- κ B/Rel-mediated regulation of apoptosis in hematologic malignancies and normal hematopoietic progenitors. *Leukemia* **18**, 11–17 (2004).
94. Dempsey, P. W., Doyle, S. E., He, J. Q. & Cheng, G. The signaling adaptors and pathways activated by TNF superfamily. *Cytokine Growth Factor Rev.* **14**, 193–209

Appendix

Table 1: Raw tumor data. Statistics were performed using a standard t-test on JMP statistical analysis program, with error taken using the 95% confidence. The outlier from the KSHV WT-infected mice was removed from the study.

Cell Type	Number of Tumors	Total Mass (g)	Cell Type	Number of Tumors	Total Mass (g)	Cell Type	Number of Tumors	Total Mass (g)
BJAB	1	5.66	WT	2	1.704	vIL6-	4	1.2713
BJAB	1	3.51	WT	7	0.5512	vIL6-	2	1.3787
BJAB	10	1.5021	WT	5	1.3784	vIL6-	1	0.9561
BJAB	10	1.6376	WT	8	4.4703	vIL6-	3	1.1491
BJAB	5	0.418	WT	4	0.435	vIL6-	4	0.6498
BJAB	9	1.0661	WT	1	0.0952	vIL6-	2	0.8614
BJAB	1	0.9125	WT	2	0.5767	vIL6-	1	1.4577
BJAB	3	1.32206	WT	2	1.4436	vIL6-	2	1.4213
BJAB	1	4.415	WT	4	0.5186	vIL6-	1	1.6854
BJAB	1	2.7748	WT	2	0.1893	vIL6-	1	1.1095
BJAB	1	4.11124	WT	1	0.6772	vIL6-	1	1.8646
BJAB	4	1.8542	WT	0	0	vIL6-	1	0.9918